

REVIEW ARTICLE | SEPTEMBER 28 2023

## Nanostructure enabled extracellular vesicles separation and detection

Xinyuan He; Wei Wei; Xuexin Duan ✉



*Nanotechnol. Precis. Eng.* 6, 045002 (2023)

<https://doi.org/10.1063/10.0020885>



Nanotechnology and  
Precision Engineering

纳米技术与精密工程



AIP  
Publishing

IF 3.7 Diamond Open Access

**No Article Processing Charges (APCs)**

Indexed by ESCI and Ei Compendex

# Nanostructure enabled extracellular vesicles separation and detection

Cite as: Nano. Prec. Eng. 6, 045002 (2023); doi: 10.1063/10.0020885

Submitted: 11 April 2023 • Accepted: 19 May 2023 •

Published Online: 28 September 2023



View Online



Export Citation



CrossMark

Xinyuan He,<sup>1</sup> Wei Wei,<sup>1</sup> and Xuexin Duan<sup>1,2,a)</sup>

## AFFILIATIONS

<sup>1</sup>State Key Laboratory of Precision Measuring Technology and Instruments, Tianjin University, Tianjin 300072, China

<sup>2</sup>Department of Chemistry, School of Science, Tianjin University, Tianjin 300072, China

<sup>a)</sup>Author to whom correspondence should be addressed: xduan@tju.edu.cn

## ABSTRACT

Extracellular vesicles (EVs) have recently attracted significant research attention owing to their important biological functions, including cell-to-cell communication. EVs are a type of membrane vesicles that are secreted into the extracellular space by most types of cells. Several biological biomolecules found in EVs, such as proteins, microRNA, and DNA, are closely related to the pathogenesis of human malignancies, making EVs valuable biomarkers for disease diagnosis, treatment, and prognosis. Therefore, EV separation and detection are prerequisites for providing important information for clinical research. Conventional separation methods suffer from low levels of purity, as well as the need for cumbersome and prolonged operations. Moreover, detection methods require trained operators and present challenges such as high operational expenses and low sensitivity and specificity. In the past decade, platforms for EV separation and detection based on nanostructures have emerged. This article reviews recent advances in nanostructure-based EV separation and detection techniques. First, nanostructures based on membranes, nanowires, nanoscale deterministic lateral displacement, and surface modification are presented. Second, high-throughput separation of EVs based on nanostructures combined with acoustic and electric fields is described. Third, techniques combining nanostructures with immunofluorescence, surface plasmon resonance, surface-enhanced Raman scattering, electrochemical detection, or piezoelectric sensors for high-precision EV analysis are summarized. Finally, the potential of nanostructures to detect individual EVs is explored, with the aim of providing insights into the further development of nanostructure-based EV separation and detection techniques.

© 2023 Author(s). All article content, except where otherwise noted, is licensed under a Creative Commons Attribution (CC BY) license (<http://creativecommons.org/licenses/by/4.0/>). <https://doi.org/10.1063/10.0020885>

## KEYWORDS

Nanostructure, Extracellular vesicle, Separation, Detection, Individual

## I. INTRODUCTION

### A. Introduction to extracellular vesicles

Cells from diverse domains of life secrete membrane-enclosed vesicles known as extracellular vesicles (EVs).<sup>1</sup> EVs carry specific protocellular components, including DNA, RNA, lipids, proteins, and metabolites.<sup>2,3</sup> These components mediate intercellular communication, especially in oncology.<sup>4</sup> EVs participate in cell-microenvironment interactions and influence cell proliferation, migration, immune regulation, pregnancy, and cardiovascular diseases, among other conditions.<sup>5</sup> EVs are ubiquitous in various human body fluids such as blood, saliva, semen, sputum, urine,

cerebrospinal fluid, amniotic fluid, and breast milk.<sup>6</sup> EV formation involves a complex process in which cells endocytose cell surface proteins and extracellular soluble proteins to form early endosomes (ESEs). ESEs mature into late endosomes (LSEs), which eventually become multivesicular bodies (MVBs). MVBs fuse with the plasma membrane and release their intraluminal vesicles (ILVs) as EVs by exocytosis.<sup>7</sup> EVs are classified into exosomes, microvesicles (MVs), and apoptotic bodies based on their origin and size.<sup>8</sup> Exosomes are small lipid bilayer vesicles with an average thickness of about 5 nm, derived from MVBs with diameters of 30–150 nm and densities of 1.08–1.22 g/ml.<sup>9</sup> MVs have diameters of 50–1000 nm and densities of 1.12–1.16 g/ml, and they bud directly from the outer plasma

membrane. Apoptotic bodies have diameters of 500–5000 nm and are secreted by apoptotic cells during the late stages of programmed cell death.<sup>10</sup>

In recent years, EVs have attracted much research interest. EVs carry specific biomarkers, such as tetraspanins (CD9, CD63, and CD81), integrins, immunomodulatory proteins, and nucleic acids [DNA, mRNA, and microRNA (miRNA)].<sup>11</sup> These biomarkers act as a biological fingerprint of the source cell, reflecting its biological information.<sup>12</sup> EVs are intimately involved in tumor initiation, proliferation, and metastasis.<sup>7,13,14</sup> Studies have shown that tumor cells secrete more EVs than normal tissue cells.<sup>15,16</sup> The proteins and nucleic acids in EVs differ not only between cancer patients and healthy individuals, but also at different stages of cancer or other disease.<sup>17,18</sup> Therefore, EVs are potential biomarkers for early diagnosis and prognosis of cancer and other diseases and have great clinical diagnostic value.<sup>19,20</sup> Dash *et al.*<sup>21</sup> explored the potential of plasma EV membrane proteins from tumor cells as biomarkers for early colorectal cancer (CRC) detection. They found that the expression levels of ADAM10, CD59, and TSPAN9 were 2.19–5.26-fold higher in plasma EVs of CRC patients. Li *et al.*<sup>22</sup> examined circular RNA (circRNA) in EVs secreted by high-grade astrocytoma. They constructed a circRNA panel of serum EVs and discovered that circRNA could serve as a liquid biopsy target for monitoring and treating high-grade astrocytoma (HGA). Moreover, EVs can be used not only for diagnosis but also for therapy. In addition, EVs are an excellent natural delivery vehicle, which can be used to load biomolecules for targeted therapy. Liang *et al.*<sup>23</sup> designed EVs derived from HEK293T cells as vectors targeting CRC cells. Anti-cancer miR-21 inhibitors were loaded onto these EVs, mediated by electroporation. It was observed that tumors were reduced in mice with colon cancer by intravenous injection of these EVs *in vivo*.

## B. Existing separation and detection techniques

Traditional techniques for separating EVs include ultracentrifugation, precipitation, immunoaffinity, ultrafiltration, and size exclusion chromatography.<sup>24</sup> Ultracentrifugation (UC) is considered the gold standard for separating EVs.<sup>19</sup> This method extracts EVs by centrifuging at low speeds (300g–2000g) and gradually increasing to high speeds (100 000g–200 000g) to separate cells, cell debris, vesicles, and proteins.<sup>25</sup> However, UC also has clear drawbacks. First, the requirement for a large sample volume (>10 ml) makes it unsuitable for processing trace biological samples.<sup>26</sup> Second, the long centrifugation time and high rotational speeds damage the integrity of EVs, potentially affecting the feasibility of their downstream analysis. This method also causes co-precipitation of proteins, leading to poor recovery.<sup>19</sup> Third, UC requires expensive equipment and trained operators, which limits its clinical application.<sup>19,26</sup>

Size exclusion chromatography (SEC) is a method that separates EVs based on their size.<sup>20,27</sup> SEC utilizes a stationary phase column consisting of spherical polymer porous beads with varying pore sizes to separate EVs.<sup>10,28</sup> This technique enables smaller EVs to enter the pores and be eluted with phosphate-buffered saline (PBS), while larger EVs cannot diffuse into the pores and move between the porous beads. Compared with UC, SEC does not require expensive equipment, it is easy to operate, and it separates EVs more completely.<sup>29</sup> However, contaminants such as lipoprotein may still

remain in the EVs after separation.<sup>30</sup> Furthermore, the SEC stationary phase may interact nonspecifically with the sample, which can alter the selectivity of separation. SEC is also limited by low concentration and low size resolution.<sup>27,31</sup>

Another approach to separate EVs using solubility or dispersibility is a precipitation-based technique. Polymer or saline solution, such as polyethylene glycol (PEG), is usually used as a precipitating agent.<sup>32</sup> The polymer binds water molecules and forces poorly soluble EVs out of solution.<sup>33</sup> Precipitants and samples are incubated overnight under certain conditions, and then the precipitate containing EVs is separated by low-speed centrifugation (1500g) or filtration.<sup>34,35</sup> Finally, the residue is washed with PBS solution for further downstream analysis. Reports in the literature mention that the pH value of the EV separation environment is one of the key parameters affecting the separation quality and yield. Although this method does not require specialized equipment, is easy to use, and can handle large sample volumes, the precipitating agent interferes with downstream analysis and the precipitation process damages the membrane structure of EVs. Moreover, the co-precipitation of non-EV particles (e.g., proteins) can reduce separation efficiency.<sup>36</sup>

One of the more popular methods for separating EVs using physical properties is ultrafiltration (UF).<sup>37</sup> The working principle of UF is similar to that of traditional filtration, which is based on the size or molecular weight of particles for classification. During the filtration process, particles larger than the pore size are trapped on the membrane, while particles smaller than the pore size pass through the membrane.<sup>38,39</sup> The operational steps of UF are simple and easy, and it is time-saving and low-cost, but it also has prominent disadvantages. During the passage of EVs through the membrane pores, they will be subjected to high pressures, leading to extrusion deformation, which can result in morphological changes or damage, thus interfering with downstream analysis.<sup>40</sup> Also, the membrane will become clogged after filtration, both by large particles on the membrane surface and by small particles inside the membrane pores, resulting in a decrease in flux and a decrease in recovery.<sup>41</sup>

The immunoaffinity method relies on interaction between antigen and antibody or between receptor and ligand to separate EVs.<sup>10,27</sup> This technique is supported by abundant antigen markers on the membrane surface of EVs, such as CD9, CD63, CD81, and others.<sup>25,42</sup> A common approach is to immobilize specific antibodies on magnetic beads, chromatographic matrices, multi-well plates, and microfluidics to capture EVs.<sup>43,44</sup> Immunoaffinity-based chromatography methods resemble traditional chromatographic separations by immobilizing antibodies in the stationary phase and EVs in the mobile phase. Different components in the sample can be separated by exploiting their different elution rates.<sup>45</sup> Some literature reports indicate that the immunoaffinity method has much higher capture efficiency and yield of EVs than UC.<sup>40,46</sup>

In addition, traditional detection technologies are divided into many categories, which are only listed here and not described in detail. Methods for characterizing the size and concentration of EVs include nanoparticle tracking analysis (NTA),<sup>47</sup> dynamic light scattering (DLS),<sup>48</sup> and flow cytometry (FCM).<sup>49</sup> Methods for characterizing EV morphology include scanning electron microscopy (SEM), transmission electron microscopy (TEM), and

atomic force microscopy (AFM).<sup>37</sup> Enzyme-linked immunosorbent assay (ELISA)<sup>50</sup> and immunoblotting are used to characterize the types of proteins contained in EVs.<sup>51</sup> Methods for detecting RNA in EVs include quantitative reverse transcription polymerase chain reaction (qRT-PCR). In addition, surface plasmon resonance (SPR) imaging,<sup>52</sup> tunable resistive pulse sensing (TRPS),<sup>53</sup> laser tweezers Raman spectroscopy (LTRS),<sup>54</sup> and other methods are used for EV detection.

In the past decade, researchers have developed a variety of commercial instruments or kits to separate and detect EVs from cell cultures or body fluids.<sup>55</sup> However, owing to the complex composition of biological samples and where EV components intersect in density and size range, most available methods cannot accurately isolate or analyze specific constituent parts of EVs—particularly proteins and nucleic acids.<sup>56,57</sup> Consequently, most of the EV-related research literature currently available is typically based on mixed subsets of EVs secreted by different cells, including additional EV components and biologically active acellular components. Therefore, the true nature of EVs with their specific functions and structural dimensions has been challenging to elucidate clearly, thus hindering the investigation of their biological and clinical applications.<sup>24</sup> The limitations of the methods mentioned above have brought significant challenges to the development of EV separation and detection techniques.

Advances in nanotechnology and micro- and nanoprocessing techniques have enabled the production of nanostructures that are precisely sized to fit EVs. Incorporating these structures into microfluidic chips increases the EV exposure probability by expanding the surface area available. Nanostructures not only provide higher separation efficiency, purity, and throughput for EV separation, but also enable enhanced accuracy, specificity, and sensitivity through nanoscale detection.<sup>58–60</sup> Through nanotechnology, researchers have designed a variety of functional nanostructures

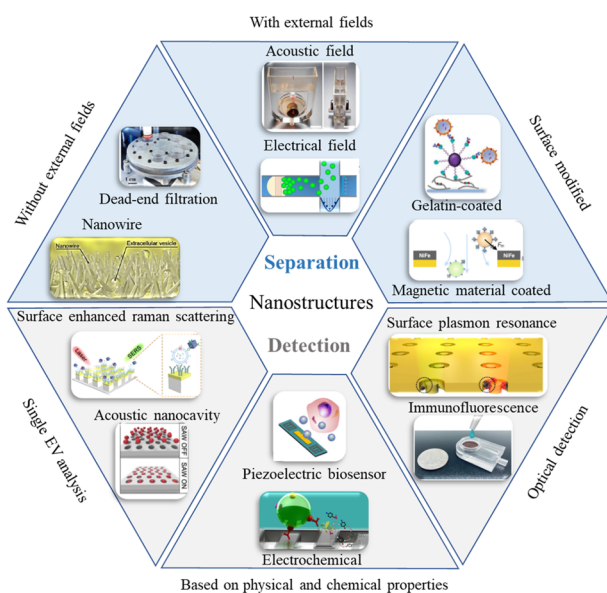
with the advantages of low sample consumption, low cost, and portable operation. The combined advantages of nanotechnology and microfluidic technology provide precious resources for obtaining suitable EV samples for further research and clinical application. Although microfluidic systems for separating and detecting EVs are still in their infancy, the fusion of nanotechnology and microfluidics has achieved outstanding results. In this review, we first divide the nanostructures used to separate EVs into three categories, namely, nanostructures without external field, nanostructures with an external field, and surface-modified nanostructures, and we review the development of nanostructure-based separation methods in typical examples of biomedical and clinical analysis. Second, we introduce the nanostructure-based EV detection methods and review the innovative applications of nanostructures in the detection field. Third, we review the capture and detection of individual EVs based on nanostructures, fully demonstrating the advantages of nanostructures in the analysis of individual EVs (Scheme 1). In each section, we will introduce the principles and mechanisms in detail and provide an in-depth analysis of their advantages and challenges. Finally, we discuss the future development trends of nanostructures and their potential applications in biomedical fields.

## II. NANOSTRUCTURE-BASED EV SEPARATION METHODS

The separation of EVs based on nanostructures is an emerging technique that is compatible with microfluidic chips to create nanoscale lab-on-a-chip devices. Nanostructures provide a high area-to-volume ratio, increasing the contact probability with EVs, and requiring smaller sample volumes with fewer reagents. This approach also eliminates the need for the bulky equipment required by conventional methods, since it combines multiple separation methods and components on a single chip. Techniques for separating EVs based on nanostructures are classified according to whether they use physical properties or biological characteristics. Physical property-based mechanisms use nanostructures with or without external fields, taking advantage of EV density, size, and electrical properties. Such microfluidic platforms rely on filtration, nanowires, acoustics, deterministic lateral displacement, and electricity. Meanwhile, biological property-based separation relies on specific interactions of EV surface biomarkers with capture agents. These approaches employ immunoaffinity-based antibodies or aptamers, as well as polymeric reagents.

### A. Nanostructure without external fields

Generally speaking, the platforms based on microfluidics combined with nanostructures without external fields use pressure or centrifugal force to achieve the separation of EVs. These platforms rely on differences in physical properties to separate different kinds of EVs.<sup>24,58</sup> According to the current literature, exosomes typically range in diameter from 30 to 150 nm and have densities ranging from 1.08 to 1.22 g/ml.<sup>9</sup> Nanostructures without external fields separate EVs with the same physical properties, sacrificing purity while improving size resolution, and thus the requiring further downstream analysis.<sup>61</sup> In this subsection, we will introduce platforms to achieve separation based on the above EV physical properties,



SCHEME 1. Nanostructure-based EV separation and detection methods.



divided into (1) the dead-end filtration method, (2) the tangential flow filtration method, (3) the nanowire filtration method, and (4) the nanoscale deterministic lateral displacement (nano-DLD) method (Table I).

### 1. Dead-end filtration method

Dead-end filtration is a classic filtering mode often used in a variety of application scenarios. Particles and solutions smaller than the membrane pore diameter pass through the membrane, while particles larger than the pore diameter are trapped on the membrane.<sup>62</sup> There are two ways to create the required pressure difference: the first is to add positive pressure upstream of the membrane (i.e., at the inlet), and the second is to add negative pressure downstream of the membrane (i.e., at the outlet). Combining two or more membranes can be used for sequential filtration to remove large particles and proteins, thereby retaining EVs in a specific size range.<sup>63</sup>

On a microfluidic-based filtration platform, Liang *et al.*<sup>14</sup> developed an integrated dual-filter microfluidic device to separate EVs from the urine of bladder cancer patients [Fig. 1(a)]. The device contained polymethyl methacrylate (PMMA) layers with two fixed polycarbonate (PC) membranes of sizes 200 and 30 nm, respectively. Subsequent to positive pressure filtration, microbeads and particles exceeding 200 nm were trapped on the larger membrane, while nucleic acids and proteins below 30 nm passed through the smaller one, enabling EV retention. Anti-CD63 antibody labeled and formed an immune complex with EVs, which was followed by interaction with streptavidin–horseradish peroxidase (SA-HRP), leading to on-chip separation, enrichment, and quantification of EVs in urine. The nonspecific adsorption of EVs on the membrane surface in such as device may reduce the recovery rate. As a result,

the membrane surface becomes clogged, decreasing filtration efficiency. Also using a dual-filtration system, Dong *et al.*<sup>64</sup> devised an integrated microfluidic chip named ExoIDChip for efficient separation and high-sensitivity detection of EVs [Fig. 1(b)]. The chip had a slidable mechanical structure connecting two fluid channels. After completion of filtration in the left channel, the upper channel was moved to the right, and the excess AptCD63 aptamer passed through. Enrichment of unbound aptamers was performed by photonic crystal nanostructures, which enhanced fluorescence when bound to nitrocellulose membranes. In the final detection stage, infused SA-HRP quantified EVs by a competitive immunoassay, enabling sensitive EV detection. The photonic crystal nanostructure had a fluorescence enhancement effect. ExoID-Chip was used to differentiate serum samples from breast cancer patients and healthy individuals.

On the basis of the dead-end filtration method, Liu *et al.*<sup>63</sup> developed a new type of filter chip called ExoTIC [Fig. 1(c)]. This used PC membranes with different pore sizes as filters to separate EVs from different clinical samples of blood, lungs bronchoalveolar lavage fluid, cell culture medium, saliva, and urine. On this platform, the membranes were modularized to allow easy connection to syringes and syringe pumps. After filtration for some time, the device was rotated through 180° to prevent clogging from causing a drop in flux. ExoTIC gave a four times higher yield than UC, and a three to four times higher yield than a PEG precipitation kit, with a separation efficiency exceeding 90%. Furthermore, it was possible to separate EV subpopulations in different size ranges by cascading together filters of different sizes (e.g., 30, 50, 80, 100, and 200 nm).

Seder *et al.*<sup>65</sup> fabricated an automated non-microfluidic platform [Fig. 1(d)]. The working principle of this platform was similar to that of ExoTIC, cascading membranes with different pore sizes (30, 50, 80, 100, and 200 nm) and using positive pressure to filter

TABLE I. Nanostructure-based EV separation method without external fields.

EV separation method	Separated size (nm)	Purity (%)	Recovery yield (%)	Throughput (μl/min)	Reference
<i>Dead-end filtration:</i>					
Dual-filter microfluidic device	~155	NA	74.2	40	14
ExoIDChip	~20–200	NA	NA	10	64
ExoTIC	~30–100	75	>90	~83	63
Movable-layer device	~30–200	NA	89	~13	65
<i>Tangential flow filtration:</i>					
Exodisc	~20–600	55	>95	36	68
Exo-Hexa	~20–450	83	>95	133	67
Serpentine channel device	~100	>97	80	50	70
Ultrathin silicon nitride nanomembrane	~80	NA	17.2	5	71
<i>Nanowire separation:</i>					
Ciliated microcolumn arrays	~83–120	NA	45–60	10	38
Nanowire-induced electrostatic collection	~30–200	>99	NA	50	74
3D carbon nanotube arrays	~80–300	NA	47–55	200	75
<i>Nanoscale deterministic lateral displacement (nano-DLD):</i>					
Nano-DLD sorting using pillar array	<100	NA	99	0.0001–0.0002	76
Nano-DLD sorting	~30–200	NA	~50	15	77
i-nanoDLD	~20–1000	>95	NA	~283	85

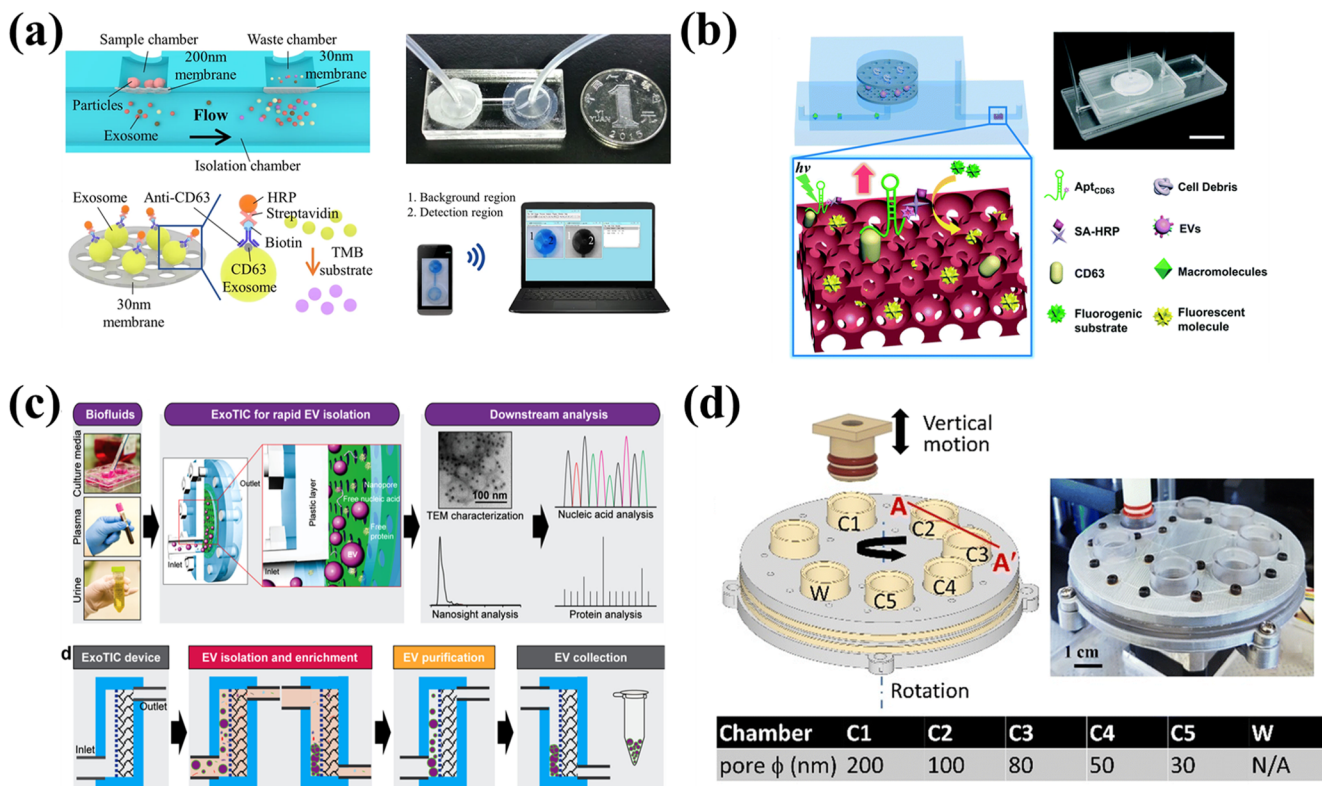


**FIG. 1.** Platforms for EV separation using dead-end filtration. (a) Microfluidic dual-filtration platform for EV separation.<sup>14</sup> Reproduced from Liang *et al.*, *Sci. Rep.* **7**, 46224 (2017). (b) Schematic of the ExoDchip.<sup>64</sup> Reproduced from Dong *et al.*, *Lab Chip* **19**, 2897–2904 (2019). (c) Schematic and workflow of ExoTIC.<sup>63</sup> Reproduced from Liu *et al.*, *ACS Nano* **11**, 0712–10723 (2017). (d) EV separation device with a vertically moving piston and a rotating chip to separate EVs according to their sizes.<sup>65</sup> Reproduced from Seder *et al.*, *Lab Chip* **22**, 3699–3707 (2022).

EVs. The main structure of this automatic device was composed of a vertically movable piston and a rotatable disc. Seven open chambers were distributed on the disk, with each chamber being connected by a microchannel and a one-way valve, which also contained PC membranes with different pore sizes. Experiments with this device showed that when the piston was pressurized at a speed of 5  $\mu\text{m/s}$ , EVs did not deform significantly. Compared with UC, the purity of the isolate was ten times higher, and the recovery rate was as high as 89%. The results of EV characterization showed that the greater the number of EVs secreted by the cells, the higher were the expressions of CD63 protein and TSG101 protein. It was found that the device could separate EVs with different sizes of 30, 50, 80, 100, and 200 nm at high resolution and could separate EV subpopulations according to size.

Although dead-end filtration has a simple structure, easy operation, and low cost, as the filtration time becomes longer, large particles will accumulate on the membrane, forming a cake structure and causing membrane pollution. The cake will cause the filtration resistance to increase continuously, the permeability of the membrane will decrease, and this will eventually lead to failure of separation. In addition, higher pressures may damage the integrity of EVs.

## 2. Tangential flow filtration method

Tangential flow filtration (TFF) is a filtration method where the flow direction of the sample is perpendicular to the filtration direction, so that the shear force of the tangential fluid reduces the accumulation of large particles on the membrane surface.<sup>66</sup> TFF equipment has been developed, such as LabSpinner's lab-on-a-disc, which uses centrifugal force to achieve TFF.<sup>67</sup> Woo *et al.*<sup>68</sup> developed Exodisc for label-free, rapid, and sensitive EV separation and detection. This platform enabled fully automated EV separation of 1 ml samples within 30 min from cell culture supernatant (CCS) or cancer patient urine, with the sample being under a centrifugal force (about 500g) much less than that in UC. The sample passed successively through two membranes, with the combination of a 20 nm anodic aluminum oxide (AAO) membrane and a 600 nm PC membrane proving most suitable. Microvalves automatically controlled different chambers, and the 20 nm AAO membrane was able to filter out protein. Although EV recovery from CCS was found to be greater than 95%, the purity of the EVs was affected by co-segregation of larger EVs (size range 200–600 nm) [Fig. 2(a)]. Subsequently, the same group made adjustments to Exodisc and developed Exodisc-B.<sup>69</sup> With this, they were able to enrich EVs from whole blood samples with a volume of 30–600  $\mu\text{l}$  within 40 min. The device had a

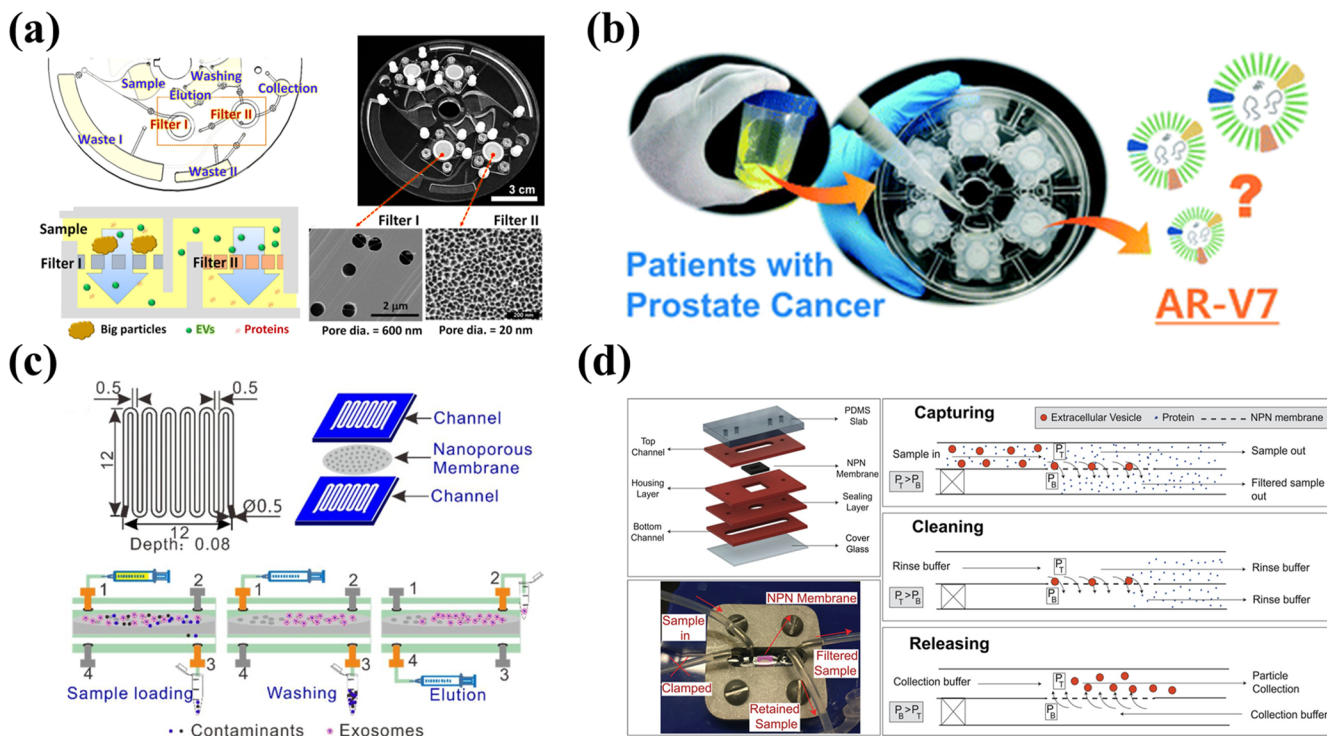


**FIG. 2.** Platforms for EV separation using tangential flow filtration. (a) Schematic of Exodisc.<sup>68</sup> Reproduced from Woo *et al.*, ACS Nano. **11**, 1360–1370 (2017). (b) Schematic of Exo-Hexa.<sup>67</sup> Reproduced from Woo *et al.*, Lab Chip **19**, 87–97 (2019). (c) Tangential flow filter with serpentine microchannels.<sup>70</sup> Reproduced from Han *et al.*, Sensors Act. B Chem. **333**, 129563 (2021). (d) Ultrathin silicon nitride membrane filtration system.<sup>71</sup> Reproduced from Dehghani *et al.*, Adv. Mater. Technol. **4**, 1900539 (2019).

capture efficiency of 75% at a lower centrifugal force (66g). Furthermore, Exodisc extracted mRNA from EVs with a 100-fold increase compared with UC.<sup>68</sup> Finally, on-chip ELISA was used to detect EVs from the urine of bladder cancer patients and showed high levels of CD9 and CD81 expression. This platform is clinically significant for detecting EVs in urine for cancer diagnosis. In 2019, Woo *et al.*<sup>67</sup> developed Exo-Hexa, which had an improved chamber structure compared with Exodisc, increasing the purity of the isolate from 55% to 83%. Throughput, was also improved with this device, with one disc being able to process six samples simultaneously [Fig. 2(b)].

Apart from centrifugal force, the driving force of tangential flow can also be provided by a syringe pump or a vacuum pump. Han *et al.*<sup>70</sup> successfully separated and purified EVs from human blood using tangential flow via a symmetrical two-layer PMMA serpentine flow channel and a 100 nm PC membrane, which separated over 97% of protein and other impurities. The collected EVs were analyzed using matrix-assisted laser desorption/ionization time-of-flight (MALDI-TOF) mass spectrometry (MS), proving effective clearance of plasma proteins, with only the protein spectrum of EVs present [Fig. 2(c)]. Dehghani *et al.*<sup>71</sup> developed a tangential flow analyte capture (TFAC) EV separation and purification method using an ultrathin silicon nitride nanomembrane of 10  $\mu\text{m}$  thickness and 80 nm pore size to increase capture efficiency and avoid cake formation, reducing pressure drop. Compared with PC membranes, ultrathin silicon nitride membranes demonstrate low clogging and transmembrane pressure drop, sustaining continuous filtration for

a longer period while also enhancing the separation and release efficiency of EVs. The device also supported *in situ* EV analysis, outperforming dead-end filtration [Fig. 2(d)].

### 3. Nanowire separation method

Nanowires represent another size-based technology that leverages the physical properties of EVs for separation by integrating mechanical structures into microfluidic platforms. A prime example of nanowire implementation is an EV filtration system comprising a structural array of ciliated microcolumns, developed by Wang *et al.*<sup>38</sup> This configuration possessed hierarchical filtration capability [Fig. 3(a)]. Traditional micromachining techniques were used to fabricate a microcolumn array on a silicon substrate, permitting the use of an electrodeposited silver nanoparticle catalyst in electroless etching on the sidewall of the microcolumn, finally causing cilia formation. Since the spacing of the nanowires was adjustable, ranging from 30 to 200 nm, this enabled the capture of EVs within the corresponding size range (40–100 nm). Furthermore, EVs could be retrieved without damaging the nanowires, by soaking them in PBS solution.<sup>38</sup> However, owing to its low throughput, this platform had limited prospects for practical application. Rahong *et al.*<sup>72</sup> fabricated a 3D nanowire structure embedded in a PDMS microchannel via a bottom-up approach, allowing them to grow tin oxide nanowires with an average diameter of 18.9 nm on a quartz substrate. This method was able to quickly separate biomolecules, such as proteins, DNA, and RNA. The concentration of EVs in urine is extremely



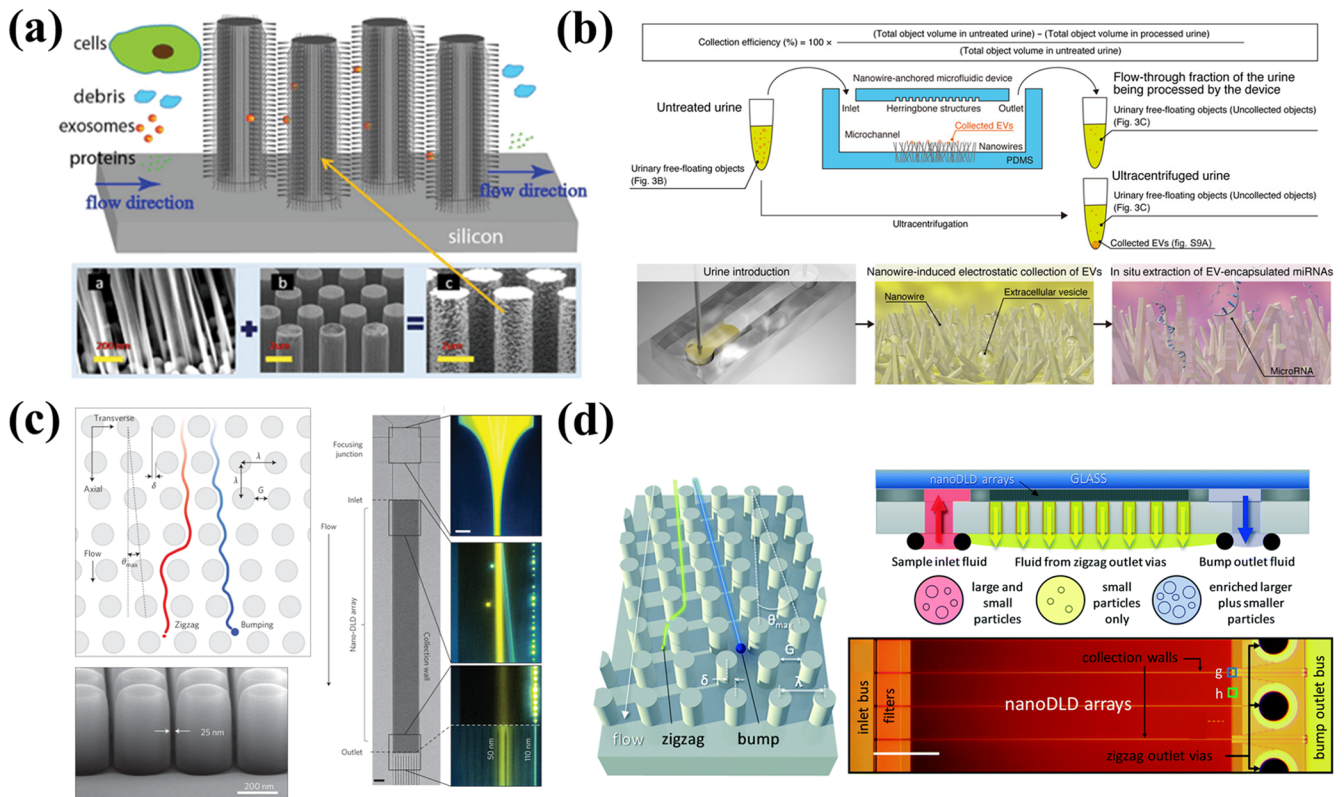


**FIG. 3.** Platforms for separating EVs based on size. (a) EV filtration system composed of ciliated microcolumn arrays that is capable of hierarchical filtration.<sup>38</sup> Reproduced from Wang *et al.*, *Lab Chip* **13**, 2879–2882 (2013). (b) Microfluidics of ZnO nanowires for separation of low-concentration EVs from urine.<sup>74</sup> Reproduced from Yasui *et al.*, *Sci. Adv.* **3**, e1701133 (2017). (c) Nanoscale micropillar array chips with gap sizes ranging from 25 to 235 nm.<sup>76</sup> Reproduced from Wunsch *et al.*, *Nat. Nanotechnol.* **11**, 936–940 (2016). (d) Chip composed of 1024 parallel nano-DLD arrays.<sup>77</sup> Reproduced from Smith *et al.*, *Lab Chip* **18**, 3913–3925 (2018).

low, posing specific challenges to EV extraction.<sup>73</sup> To address this, Yasui *et al.*<sup>74</sup> used a device composed of zinc oxide nanowires and herringbone substrates immobilized in a microchannel to efficiently separate low-concentration EVs from 1 ml urine [Fig. 3(b)]. They verified that urine EVs carried a negative charge, while nanowires displayed a positive charge at pH 6–8, thus increasing EV capture efficiency. Consequently, within 40 min of *in situ* extraction of miRNAs, an improvement compared with UC and commercially available kits, this platform was able to harvest ~1000 types of miRNAs.

Besides utilizing nanowires, researchers have also employed carbon nanotubes for the separation of EVs. Yeh *et al.*<sup>75</sup> reported a microfluidic platform consisting of 3D carbon nanotube arrays that separated differently sized EVs in a label-free and high-throughput manner. These arrays were made up of 3D nitrogen-doped carbon nanotubes (CNxCNTs) that formed two regions with different pitches, capturing larger (~300 nm diameter) and smaller (~80 nm diameter) EVs. However, both types of EVs had low capture rates. In summary, while separating EVs using nanowires or carbon nanotubes offers label-free and highly efficient separation benefits, the manufacturing process can be complex, and issues with clogging also pose a challenge for this technique.

#### 4. Nanoscale deterministic lateral displacement method (nano-DLD)

Deterministic lateral displacement (DLD) is a fluid dynamics-based method through which particles of varying sizes are separated according to differences in their trajectories between periodically spaced micropillars.<sup>78</sup> This method uses rectangular, circular, or triangular arrays of micropillars distributed throughout the channel of a microfluidic chip.<sup>78,79</sup> Nano-DLD involves setting the distance between the microcolumns at the nanoscale to achieve higher separation accuracy and resolution. The critical cutoff diameter (critical dimension) of DLD is determined by the distance between micropillars and the displacement angle, which refers to the ratio of the lateral offset of the micropillar array to the center-to-center distance between two pillars. While particles smaller than the critical size exhibit a zigzag pattern as they pass through the array of micropillars, larger particles undergo lateral displacement due to the collision mode.<sup>79</sup> Nano-DLD facilitates the separation of particles that are larger and smaller than the critical size along the direction of fluid motion. The DLD technique has been employed to separate circulating tumor cells (CTCs),<sup>80</sup> blood cells,<sup>81</sup> bacteria,<sup>82</sup> and EVs.<sup>83</sup> Santana *et al.*<sup>83</sup> designed a DLD platform to study the separation of EVs from the culture supernatant of cancer cells. Their experi-

ments revealed that particles larger than the critical size (250 nm) displayed lateral displacement, while those smaller than 250 nm exhibited minimal lateral displacement. Although the efficiency of particle recovery from this microfluidic platform was only about 39%, its purity was 98.5%. However, owing to diffusion, this non-nanostructured device faced difficulties in accurately separating EVs with a diameter less than 200 nm. To effectively separate EVs, nanostructures featuring smaller gaps and finer structures or external field-assisted separation measures are necessary. Zeming *et al.*<sup>84</sup> exploited an electrostatic force in conjunction with adjustments to the ionic strength of the solution. This allowed them to achieve the separation of particles measuring 51 and 190 nm by modifying the electrostatic force between the particles and microcolumns. Wunsch *et al.*<sup>76</sup> developed a nano-DLD technique that exploited a passive microfluidic action instead of relying on an external field. They created nanoscale micropillar arrays on silicon substrates with gap sizes ranging from 25 to 235 nm [Fig. 3(c)]. Their experiments revealed that at low Péclet numbers  $Pe$ , where deterministic displacement and diffusion compete, the resolution of the nano-DLD arrays was adequate enough to separate particles sized between 20 and 110 nm. Although the platform had the potential to separate biocolloids on a chip, the flow rate remained limited to 0.1–0.2 nl/min. To address the challenge of sample throughput, Smith *et al.*<sup>77</sup> transformed a single-array nano-DLD device into a parallel array comprising 1024 separate nano-DLD arrays integrated on a single chip [Fig. 3(d)]. Following calibration with fluorescent particles, intact EVs were successfully separated from human serum and urine. The platform demonstrated a recovery rate of 50%, surpassing conventional techniques such as UC and SEC. Wunsch *et al.*<sup>85</sup> developed i-nanoDLD, an integrated nano-DLD device. They fabricated 31 160 parallel arrays at high density, resulting in a throughput of 17 ml/h, a first for this technique. They then utilized the device to enrich and purify EVs smaller than 200 nm from urine, significantly reducing protein content and other impurities. While the recovery rate of the

nano-DLD technique is high, its clinical applicability is limited by the complexity of the manufacturing process, and crucial concerns remain regarding equipment clogging and co-precipitation of EVs and proteins.

## B. Nanostructure with external fields

Integrating acoustic and electric fields into nanostructures provides higher-throughput separation techniques that do not harm EVs (Table II). The acoustic field is comparable to some medical ultrasound techniques and can efficiently separate biological particles of interest.<sup>86</sup> Electric fields typically exploit the electrical properties of EVs. The zeta potential of EVs differs slightly depending on their origin, with EVs from plasma and those from breast cancer cells (MCF-7) displaying zeta potentials of approximately  $-11$  and  $-13.4$  mV, respectively.<sup>87,88</sup> These property differences facilitate the separation of EVs.

### 1. Acoustic field

The combination of an acoustic field with nanotechnology provides a label-free, reagent-free, and contact-free EV separation method. Acoustic field methods perform separation based on differences in mechanical properties such as size, density, or compressibility.<sup>89,90</sup> This approach enhances cell and bioparticle manipulation accuracy while maintaining biocompatibility.<sup>86</sup> The sample solution is subjected to acoustic streaming effects when acoustic waves are applied, allowing the acoustic radiation force and acoustic drag force to act on particles.<sup>91–93</sup> Nanostructures such as microtips, microcolumns, and filter membranes have been paired with acoustic waves to achieve EV separation functionality. Chen *et al.*<sup>94</sup> developed an ultrafast EV separation device called EXODUS by combining piezoelectric transducers (PZTs) with porous alumina (AAO) membranes. This device utilized a negative-pressure oscillation system and a double-coupled harmonic oscillation

TABLE II. Nanostructure-based EV separation method with external fields.

EV separation method	Separated size (nm)	Purity (%)	Recovery yield (%)	Throughput ( $\mu$ l/min)	Reference
<i>Acoustic field:</i>					
EXODUS	~30–200	99	90	1000	94
<i>Electrical field:</i>					
Pressure-driven filtration	~150	NA	>1.5	1	95
Electrophoretic separation on nanoporous membrane	~10–400	84	65	20	96
ExoSMP	~30–120	90	94.2	10	103
Ion-depletion zone sorting	~30–200	NA	98	1	104
Electric field-driven filtration	<150	NA	60–80	150–200	97
<i>Surface modified nanostructures:</i>					
Fe <sub>3</sub> O <sub>4</sub> magnetic nanoparticles coated with PEG	~30–200	~60	NA	NA	108
ExoTENPO	~150	NA	NA	~166	109
Wedge-shaped nanopore	~30–400	NA	85%	~83	110
Peptide-modified ZnO nanowires	~80–160	NA	70	50	111
NanoVilli	~30–300	NA	63–82	~3	112
Magnetic polypyrrole nanowire	~40–150	NA	NA	~4	113
Y-shaped micropillars	~185	NA	83	50	114



system to generate high- and low-frequency vibrations. EXODUS not only effectively circumvented the clogging problem caused by the accumulation of proteins or large vesicles on the membrane surface, but also provided enhanced purification and separation efficiency. Moreover, compared with traditional EV separation methods, this platform displayed significant improvements in processing throughput (1 ml/min), purity (99%), and recovery (90%). EVs were extracted from the urine of 113 patients displaying urinary system diseases via RNA sequencing analysis using EXODUS, demonstrating its high efficiency, effectiveness, and repeatability [Fig. 4(a)].

## 2. Electric field

In a homogeneous electric field, only charged particles migrate toward oppositely charged electrodes, leaving neutral and uncharged particles unaffected by the electric field forces.<sup>98</sup> When a particle is in a nonuniform electric field, it becomes polarized, inducing a directional movement under the dielectrophoretic (DEP) force, irrespective of the particle's charge state.<sup>99,100</sup> Generally, the magnitude of the DEP force is affected by the volume, dielectric constant, electrophoretic mobility, and electric field intensity of a particle.<sup>87,101</sup>

In EV separation methods based on the DEP effect, EVs are also subjected to thermal effects caused by the electrodes. To avoid direct contact occurring between electrodes and EVs, Ibsen *et al.*<sup>102</sup> used 400 alternating current electrokinetic (ACE) electrodes on a microfluidic platform. They overlaid the electrodes with a porous hydrogel layer, enabling concentration of larger cells and EVs under

a low field strength and the effective recovery of separated EVs. Nanostructures such as membranes can also effectively minimize the contact between electrodes and EVs. Davies *et al.*<sup>95</sup> developed a filtration system based on a pressure-driven tangential flow filtration method along with a DC electrophoresis drive for efficient separation of EVs from whole blood samples collected from melanoma mice [Fig. 4(b)]. They synthesized a porous polymer monomer (PPM) into membrane structures and integrated these within PMMA microfluidic channels via *in situ* photolithography. On application of a DC voltage, the separation of EVs based on their distinct differences in electrophoretic mobility compared with proteins increased both the purity and efficiency of the separated EVs and enabled greater extraction of RNA. Cho *et al.*<sup>96</sup> proposed an electromigration-based EV separation technique [Fig. 4(c)]. They employed an electrical field together with a dialysis membrane, featuring a pore size of 30 nm, to extract EVs from diluted mouse blood samples. pH and solution osmolarity buffers were employed to prevent the potential problems caused by Joule heating and electrochemical reaction products. The platform extracted ~65% of the EVs and excluded about 84% of the related proteins. Chen *et al.*<sup>103</sup> developed a microfluidic platform (ExoSMP) based on a dual filter device driven by an electrical field to separate EV subpopulations via size-selectivity. Mogi *et al.*<sup>104</sup> proposed a separation mechanism based on electrophoresis and employing a microfluidic chip design, utilizing a synthetic Nafion membrane sandwiched between two channels. Cations were drawn into this membrane, ultimately generating an ion-depletion region that imposed an electric field force

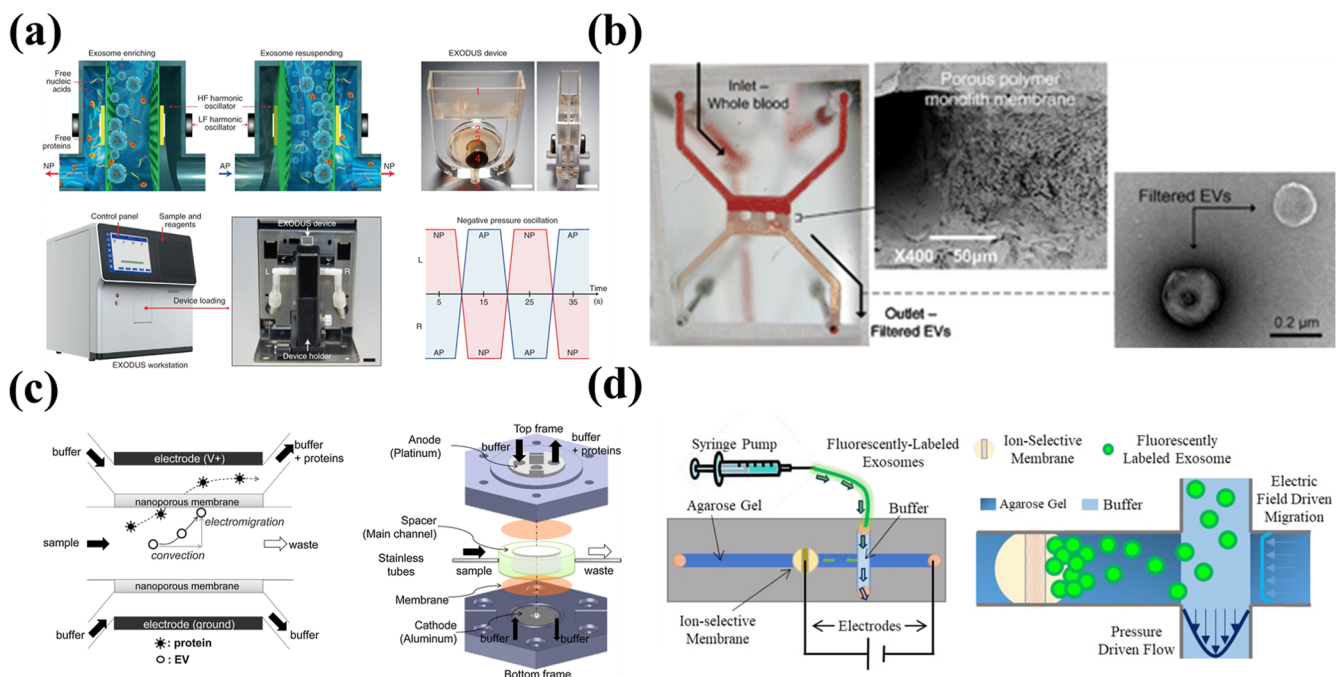


**FIG. 4.** Nanostructures combined with external fields for EV separation. (a) Schematic of the EXODUS device.<sup>94</sup> Reproduced from Chen *et al.*, *Nat. Methods* **18**, 212–218 (2021). (b) Platform for the separation of EVs by synthesizing porous membranes combined with electric field filtration in microfluidic channels.<sup>95</sup> Reproduced from Davies *et al.*, *Lab Chip* **12**, 5202–5210 (2012). (c) Electromigration-based EV separation chip.<sup>96</sup> Reproduced from Cho *et al.*, *Sensors Actuators B Chem.* **233**, 289–297 (2016). (d) Microfluidic platform combining ion-exchange membrane and gel electrophoresis.<sup>97</sup> Reproduced from Marczak *et al.*, *Electrophoresis* **39**, 2029–2038 (2018).

on EVs, resulting in their concentration within the main channel of the sample batch. Marczak *et al.*<sup>97</sup> developed a microfluidic platform incorporating ion-exchange membranes and gel electrophoresis to separate EVs [Fig. 4(d)]. In a combination of pressure- and electric field-based approaches, agarose gel was used to filter out large-scale material such as cell debris. A lateral local electric field of 100 V/cm was applied to the sample flow within the microchannel, separating EVs from other components. Ultimately, the enriched EVs permeated the ion-exchange membranes and were separated within the agarose gels.

### 3. Surface-modified nanostructures

Immunologically based separation techniques are extensively utilized for EV separation because of their high specificity, selective character, and biocompatible compatibility.<sup>105,106</sup> In contrast to traditional immunological methods, this strategy can be applied on a microfluidic platform. Specific antibodies targeting antigen features on the EV surface can be immobilized on the surfaces of either magnetic beads or microfluidic channels. Generally, nanostructures amalgamated with magnetic nanomaterials demonstrate advantages with regard to diagnostic applications, since they can function as effective carriers or probes that capture intended EVs directly.<sup>107</sup>

Utilizing a chemical co-precipitation approach, Chang *et al.*<sup>108</sup> synthesized PEG-coated Fe<sub>3</sub>O<sub>4</sub> magnetic nanoparticles with a size of 20 nm that reduced the protein content (e.g., serum albumin and immunoglobulins) of fetal bovine serum by 39.89%, without damage to EV integrity [Fig. 5(a)]. Ko *et al.*<sup>109</sup> designed the ExoTENPO chip containing six series-connected membranes. A PC membrane including a layer of magnetic material was adopted for extracting nucleic acids, proteins, and cellular debris. By utilizing biotinylated antibodies conjugated with streptavidin-coated magnetic nanoparticles (MNPs), this innovative method successfully reduced antibody amounts at a low cost. The formation of a magnetic trap by creating a wedge-shaped nanopore edge rather than cylindrical nanopores increased capture efficiency by generating a high nanoscale magnetic field gradient. Zhang *et al.*<sup>110</sup> deposited gold and NiFe successively on track-etched membranes, forming a structure capable of detecting monopoles and dipoles and consequently elevating trapping forces by ~10 times, resulting in a 99% capture efficiency on magnetic beads functionalized with anti-rabbit IgG antibody. The device was able to separate EVs from human plasma mixed with high-density lipoproteins (HDL) [Fig. 5(b)].

The abovementioned nanowire configurations can generally be combined with immunoaffinity techniques to separate EVs. Suwatthanarak *et al.*<sup>111</sup> developed a microfluidic chip with bifunc-

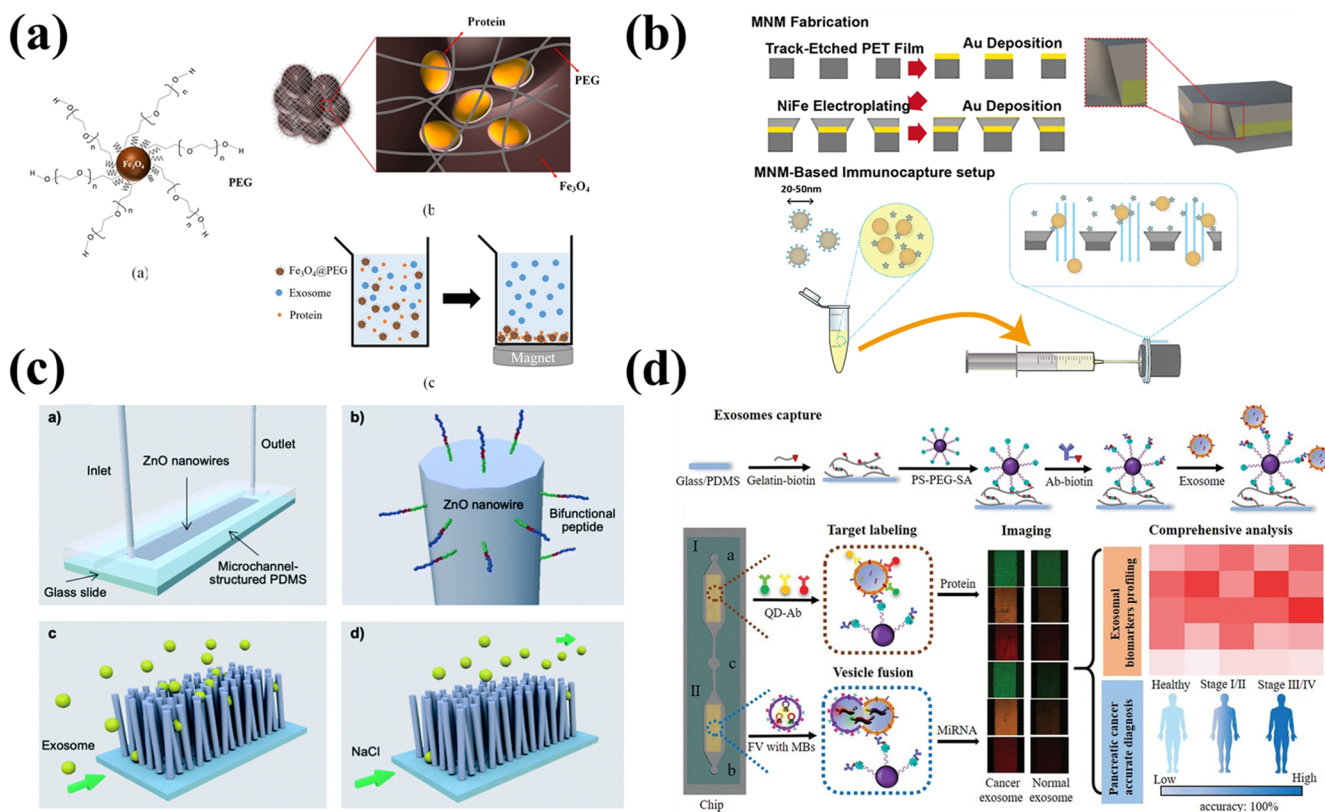


**FIG. 5.** Platforms for surface-modified nanostructures to separate EVs. (a) EV purification method using PEG-coated Fe<sub>3</sub>O<sub>4</sub> MNPs.<sup>108</sup> Reproduced from Chang *et al.*, *PLoS One* **13**, e0199438 (2018). (b) Separation of EVs and HDL by wedge-shaped magnetic nanoporous membranes.<sup>110</sup> Reproduced from Zhang *et al.*, *Commun. Biol.* **5**, 1358 (2022). (c) Microfluidic chip with bifunctional peptide-modified ZnO nanowires.<sup>111</sup> Reproduced from Suwatthanarak *et al.*, *Lab Chip* **21**, 597–607 (2021). (d) Device with Y-shaped micropillars and EV trapping through a gelatin layer and PS spheres.<sup>114</sup> Reproduced from Zhou *et al.*, *Small* **16**, 2004492 (2020).

tional peptide-modified ZnO nanowires, featuring EWI-2 amino acid sequence-functionalized arrays constructed via the bonding sequence P238. By using CD9 and CD81 markers, the chip was able to separate breast cancer cell-secreted EVs [Fig. 5(c)]. Inspired by the microvilli on the surfaces of intestinal epithelial cells, Dong *et al.*<sup>112</sup> fabricated an array of nanowires on a silicon substrate called NanoVilli. Anti-EpCAM (epithelial cell adhesion molecule) modification intensified the binding force, leading to reproducible separation of tumor cell-derived EVs from the serum of non-small-cell lungs cancer patients. Cho and co-workers<sup>113</sup> demonstrated a magnetic polypyrrole nanowire combining different types of EV antibodies with high-density MNPs. Elongated and biotinylated polypyrrole nanowires facilitated CD9-, CD63-, and CD81-specific antibody binding and consequently EV separation. Supplementing nanowires with magnetic materials or surface modification can specifically separate EVs effectively with reproducibility and convenience. However, distinguishing EV subtypes remains challenging.

Immobilizing EV-specific antibodies on the surface of microfluidic devices is another promising approach. Zhou *et al.*<sup>114</sup> designed a microfluidic platform comprising Y-shaped

micropillars. Both a biotinylated gelatin layer and streptavidin-modified polystyrene (PS) microspheres with a diameter of 50 nm were integrated into the microchannel. Utilizing the Y-shaped structure boosted the contact rate between EVs and CD63 antibodies, while the modified 50 nm PS spheres enhanced the binding sites for CD63 antibodies. Taking advantage of the thermoresponsive properties of the gelatin membrane, Zhou *et al.*<sup>114</sup> elevated the chip temperature to 37 °C to release the captured EVs [Fig. 5(d)]. Although introducing antibodies improves the capture rate of EVs, the high cost of antibodies limits their practical application, and the complicated modification process is another drawback.

### III. EV DETECTION METHODS BASED ON NANOSTRUCTURES

Nanotechnology has enabled the development of novel approaches to EV detection. Over the past few decades, numerous methods have emerged that combine nanotechnology and characterization of EVs based on their physical or biological properties. Given the complexity of components carrying EVs, detection methods tend to involve multiple techniques working in tandem to

TABLE III. Exosome detection methods based on nanostructures.

EV separation method	Limit of detection	Throughput (µl/min)	Sample	Analyte type	Reference
<i>Immunofluorescence detection:</i>					
ExoAPP	160 EVs/µl	NA	Blood	Protein	121
Peptide nucleic acid probes	NA	NA	Cell culture medium	RNA	122
MoS <sub>2</sub> multiwalled carbon nanotubes	1480 EVs/µl	NA	Blood	Protein	123
Nano-IMEX	50 EVs/µl	0.5	Plasma	Protein	124
3D herringbone nanopatterns	10 EVs/µl	0.5	Plasma	Protein	125
exoNA sensor chip	58.3 fM	~0.8–1.3	Blood	RNA	126
Integrative microfluidic device	1 EV/µl	~166	Urine	Protein	127
<i>Surface plasmon resonance (SPR) detection:</i>					
Nanowall arrays	$4.87 \times 10^7$ EVs/cm <sup>2</sup>	300	Cell culture medium	Protein	129
nPLEX	~3000 EVs	10	Ascites	Protein	130
Cu-TCPP 2D MOF	16.7 EVs/ml	5	Serum	Protein	132
APEX	200 EVs	~3	Blood	Protein	133
ExoSCOPE	1000 EVs	~0.08	Blood	Protein	134
<i>Surface-enhanced Raman scattering (SERS) detection:</i>					
Butterfly-shaped structure	30 EVs/µm <sup>2</sup>	NA	Cell culture medium	Liposome	137
Multiplex SERS detection	1 EV/µl	~2	Serum	Protein	138
3D plasmonic nanostructures	<10 aM	NA	Urine	RNA	139
Bi-functionalized SERS immunoassay	0.5 EVs/ml	NA	Serum	Protein	140
MIO structure	NA	NA	Plasma	Protein	141
<i>Electrochemical detection:</i>					
Aptasensor	10 <sup>12</sup> EVs/µl	10–400	Cell culture medium	Protein	144
Electrochemical aptasensor	954 EVs/ml	NA	Plasma	Protein	145
Aptamer strategy	70 EVs/µl	NA	Fetal bovine serum	DNA	146
Integrating nano-interdigitated electrodes	5 EVs/µl	NA	Blood	Protein	147
DeMEA chip	17 EVs/µl	0.5	Plasma	Protein	148
<i>Piezoelectric biosensor detection:</i>					
SAW sensor	1.1 EVs/µl	40	Blood	Protein	150
QCM-D	$1.4 \times 10^5$ EVs/µl	10	Serum	Protein	152



characterize EVs. Recently, EV-based point-of-care testing (POCT) techniques have been introduced, offering advanced cancer diagnosis, treatment monitoring, and assessment of prognosis. Lab-on-chip systems have been devised that incorporate nanostructures for EV separation, enrichment, purification, and detection. These systems include those based on detection using immunofluorescence, surface plasmon resonance (SPR), surface-enhanced Raman scattering (SERS), and electrochemical methods (Table III). Additionally, single-EV detection techniques have great potential for addressing the question of EV heterogeneity.

### A. Nanostructure-enabled immunofluorescence detection

Fluorescence detection is a widely used EV detection technique in biochemical analysis and clinical diagnosis, boasting high accuracy, sensitivity, and rapid response.<sup>115,116</sup> It typically works in tandem with highly specific immunoaffinity in detecting EV surface proteins or constructing surface protein maps.<sup>117</sup> EVs are frequently labeled with nonspecific lipophilic membrane fluorescent dyes such as PKH26. However, these dyes are not ideal markers for detecting and analyzing surface proteins.<sup>118</sup> Both antibodies and nucleic acid aptamers can label EV surface proteins. Given the low cost and excellent chemical stability of nucleic acid aptamers, they serve as potential substitutes for traditional antibodies in high-throughput protein analyses.<sup>119</sup> Combining fluorescent immunoassays with nanostructures facilitates the detection of EV subpopulations.

Graphene oxide (GO) is a 2D material with the capacity for fluorescence quenching. The  $\pi$ - $\pi$  stacking interaction facilitates solid affinity binding of single-stranded DNA (ss-DNA) to the GO surface, and fluorescence quenching takes place by fluorescence resonance energy between conjugated dyes and GO.<sup>120</sup> Jin *et al.*<sup>121</sup> employed GO as a nanointerface to develop ExoAPP, an EV analysis system predicated on aptamer nanoprobe. Following GO membrane quenching of specifically labeled FAM aptamers, target EVs bound these aptamers preferentially. The efficacy of both EpCAM and prostate-specific membrane antigen (PSMA) in facilitating epithelial-mesenchymal transition detection was demonstrated through identifying EVs coming from prostate cancer cells. EpCAM and CD63 were also proven to be effective in differentiating tumor-derived EVs from benign tissues [Fig. 6(a)]. Oh *et al.*<sup>122</sup> quenched FAM-labeled peptide nucleic acid probes to detect miR-193 expression in EVs, enabling precise visualization of intercellular EVs. Carbon nanotubes serve as another nanostructure. Tayebi *et al.*<sup>123</sup> employed MoS<sub>2</sub> multiwalled carbon nanotubes (MWCNTs) as a fluorescence quenching material to quench anti-human CD63PE and produced a fast, sensitive, and quantifiable EV detection platform. Following the combination of CD63PE antibody with EVs, the complex subsequently reacted with MWCNTs.

Zeng's group<sup>124</sup> devised an EV analysis platform that featured modified nanointerfaces on microchannel surfaces. For the first time, they integrated microfluidics by embedding polydopamine (PDA) films onto GO, thereby significantly increasing the deposition rate of PDA. A Y-shaped micropillar array along with the GO/PDA nanointerface structure served to elevate the contact area in the flow channel, thereby elevating EV capture efficiency

along with suppressing nonspecific adsorption. Utilizing this novel nanostructure, captured EVs were labeled using biotinylated antibodies, which subsequently underwent reaction with streptavidin-conjugated  $\beta$ -galactosidase (S $\beta$ G). The catalytic action of S $\beta$ G on 2- $\beta$ -D-galactopyranoside produces fluorescent signal amplification. This assay is ultrasensitive and elegantly detected EVs at volumes as low as 2  $\mu$ l of plasma from women suffering from ovarian cancer. Building upon their previous work, the same research group created an integrated self-assembled 3D nanopatterned microfluidic chip with highly sensitive capabilities for detecting EV surface proteins.<sup>125</sup> In this new work, the authors replaced GO/PDA with silica colloid. Nanocolloids exhibit the capability of autonomous assembly into 3D porous structures in microfluidic channels, while facilitating low hydrodynamic resistance to enable extensive EV capture and detection. The authors proceeded to employ S $\beta$ G again for enzymatic signal amplification to detect EVs. Finally, EV detection in patient plasma determined that folate receptor  $\alpha$  on EVs is a potential biomarker for early diagnosis and monitoring of ovarian cancer patients [Fig. 6(b)].

Hydrogels serve as a biocompatible materials that can be employed in the creation of nanostructures for detecting EVs.<sup>126</sup> Lim *et al.*<sup>126</sup> developed a microfluidic device, the exoNA sensor chip, to detect EV mRNA. They engineered hydrogels equipped with 3D nanostructures that enabled mRNA detection in EVs from HER2+ breast cancer mice blood within 2 h. The vacuum-driven exoNA sensor chip enabled precise control over flow rate. Their 3D nanostructured hydrogel contained two probes, ERBB2 and GAPDH, which triggered enzyme-free amplification of the fluorescent signal via *in situ* hybridization chain reaction at room temperature. Encapsulation of the probe in liposomes resulted in no fluorescent signal being generated under static conditions and ensured stability and response time during detection. Upon contact between liposomes and EVs, membrane degradation ultimately amplified the generated fluorescent signal. Comparison of mRNA expression levels between diseased mice and control groups was carried out using their platform, with outcomes that corresponded with those of qRT-PCR analysis [Fig. 6(c)].

In another study,<sup>127</sup> Liu's group proposed an integrated EV *in situ* detection device. They utilized ion sputtering to deposit gold nanoparticles on an AAO membrane to produce 50 nm nanoporous gold nanoclusters (AuNCs). Captured modified CD63 antibody was then used to hybridize EVs on the AuNCs with a secondary antibody-conjugated gold nanorod (AuR) probe. In a fluorescent field, AuNCs scatter green light, whereas AuRs scatter red. However, when the gap between the two scattered wavelengths becomes less than 200 nm, resonance coupling occurs between them, with the creation of plasmons. This shift of the spectrum of scattered light to yellow amplifies the scattering intensity. The device detected EVs directly in urine samples (500  $\mu$ l) obtained from lungs cancer patients and controls [Fig. 6(d)]. Dong *et al.*<sup>64</sup> developed a nanostructure based on a photonic crystal for EV detection. EVs were captured by an AAO nanofiltration membrane, which was then exposed to CD63-targeting aptamers (AptCD63). Some of the aptamers bound to the EVs, while the remainder passed through the membrane and were captured by a nitrocellulose membrane endowed with a photonic crystal nanostructure that boosted the fluorescent signal.

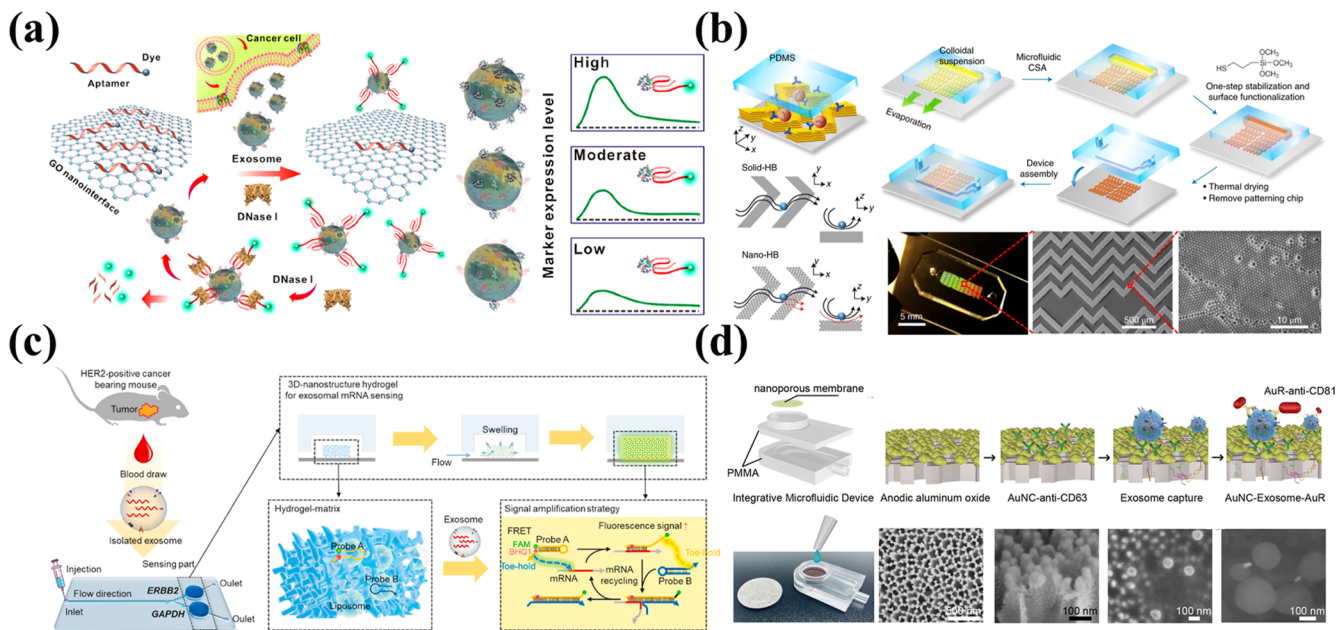


**FIG. 6.** Platforms for immunofluorescence detection of EVs. (a) Aptamer nanoprobe-based EV analysis system (ExoAPP).<sup>121</sup> Reproduced from Jin *et al.*, *Anal Chem* **90**, 14402–14411 (2018). (b) GO/PDA as a nanointerface EV analysis platform.<sup>125</sup> Reproduced from Zhang *et al.*, *Nat. Biomed. Eng.* **3**, 438–451 (2019). (c) Schematic of exoNA sensor chip.<sup>126</sup> Reproduced from Lim *et al.*, *Biosens. Bioelectron.* **197**, 113753 (2022). (d) Integrated urine EV *in situ* detection device.<sup>127</sup> Reproduced from Yang *et al.*, *Biosens. Bioelectron.* **163**, 112290 (2020).

## B. Nanostructure-enabled surface plasmon resonance (SPR) detection

Surface plasmon resonance (SPR) has emerged as an optical technique to detect molecular interactions at sensing interfaces by tracking surface refractive index fluctuations.<sup>52</sup> This technique facilitates label-free and real-time monitoring of optical contrast transformations caused by the adsorption of EVs on the plasma layer. SPR represents a novel potential approach for detecting EV subsets with increased sensitivity and specificity.<sup>128</sup>

SPR devices are ideal for EV detection owing to their sensitivity to contact responses that occur within 200 nm of the surface. Zhu *et al.*<sup>129</sup> developed nanowall array-based microfluidic chips bound to specific antibodies to extract and purify EVs from cell culture supernatants. Antibodies to CD9, glycoprotein CD41b, and the tyrosine kinase receptor MET were adhered to gold-coated glass chips and used to detect EVs through SPR imaging [Fig. 6(a)]. Weissleder's team<sup>130</sup> incorporated periodic gold nanopore arrays (nPLEX) into microfluidic chips using a light interference lithography technique to provide high-throughput and label-free EV detection through SPR. When functionalized with CD63 antibody, EVs could be detected from the ascites of ovarian cancer patients on specific binding to the nPLEX sensor. Measurement of the wavelength shift in the spectrum or of the intensity change at fixed wavelengths enabled observation of changes in the local refractive index around pore complexes, giving a limit of detection of ~3000 EVs. This technique was faster and more sensitive and required a smaller sample size when compared with the conventional gold standard ELISA. Drawing on the results of their previous work, Weissleder's team<sup>131</sup> also developed an automated detection and analysis system for EVs derived from circulating tumor cells that could diagnose

pancreatic cancer via measurement of five protein markers. This approach proved efficient, with 84% accuracy, 81% specificity, a price of only \$60, and a mere ten-minute measurement and analysis time. Chen's team<sup>132</sup> utilized a hydrothermal synthesis approach to create a 2D metal–organic framework (MOF), copper tetrakis(4-carboxyphenylporphyrin) (Cu-TCPP), which they deposited on the surface of a gold chip to provide improved optoelectronic properties. This was then used to manufacture an SPR biosensor with substantially enhanced detection accuracy, sensitivity, and quality factor. A multifunctional peptide, comprising four structural domains, was employed as a probe in an experiment to detect programmed death ligand 1 (PD-L1) EVs [Fig. 6(b)].

Shao's team<sup>133</sup> created an amplified plasma exosome (APEX) platform based on enzymatic deposition of insoluble optical precipitates and subsequent signal amplification through SPR for detection of EVs. This platform included a silicon nitride surface with a patterned array of gold nanoholes. EVs were captured on an array surface modified by CD63 antibody, displaying ~400% spectral improvement in signal by binding amyloid (A $\beta$ ). The detection of EV-bound A $\beta$  provided an improved reflection of PET imaging of plaques within the brain, enabling diagnosis of Alzheimer's disease in under an hour. Following this success, the same group increased the structural complexity of the platform by modifying the nanohole array into a nanoring array.<sup>134</sup> Using molecular reactions within a plasmonic nanoring resonator and bio-orthogonal probe amplification, in a technique they referred to as ExoSCOPE, they were able to measure EVs in the blood of a patient undergoing targeted cancer therapy, accurately classify the patient's condition, and effectively determine treatment outcomes within 24 h, representing an improvement compared



with conventional pharmacokinetic/pharmacodynamic analysis methods [Fig. 7(c)].

### C. Nanostructure-enabled surface-enhanced Raman scattering (SERS) detection

Raman spectroscopy is a molecular spectroscopy technique that relies on the inelastic scattering of photons to identify biomolecules such as nucleic acids, lipids, and proteins.<sup>135</sup> Nevertheless, the Raman signal is commonly faint owing to the minute inherent Raman scattering sizes of the molecules involved and hindrance by fluorescent signals in the target sample. By employing surface-enhanced Raman scattering (SERS) techniques to analyze coarse metal surfaces or structures, the Raman signal of the molecule being measured can be intensified ( $10^3$ – $10^{15}$ -fold), thereby improving detection sensitivity.<sup>136</sup> Consequently, an integrated microfluidic chip based on SERS techniques has the advantages of high specificity, multiplexing, and sensitivity.

For the detection of nanoscale EVs, Jalali *et al.*<sup>137</sup> devised a microfluidic platform with butterfly-shaped structure to differentiate and characterize non-immune and label-free EVs through SERS. In this approach, PS spheres were employed in bottom-up self-assembly for the manufacture of plasmonic nano-bow-tie

configurations. This structure boosted optical and electrical properties while bolstering Raman signals. EV monolayer dispersion was accomplished using the microfluidic system. A miniature portable Raman device was combined with a microfluidic chip to distinguish EVs from two different glioma cells and noncancerous glial cell EVs [Fig. 8(a)]. Wang *et al.*<sup>138</sup> reported an EPAC-II-based microfluidic chip incorporating multiplex SERS detection. This platform identified 28 serum samples (5  $\mu$ l per sample) in  $\sim$ 65 min, with an asymmetrical ring-shaped electrode formation enhancing the efficacy and sensitivity of antibody capture of EVs. Enrichment of EVs on the surface of a modified electrode through antibodies was followed by multiplex SERS detection and analysis. EV variations in sera from early-stage melanoma patients and healthy individuals were analyzed, leading to detection of high expression levels of melanoma-associated chondroitin sulfate proteoglycan (MCSP), melanoma cell adhesion molecule (MCAM), CD61, and CD63 in EVs in the former in comparison with the latter. Thus, on the basis of these four selected biomarkers, early-stage melanoma patients were successfully distinguished from healthy individuals [Fig. 8(b)].

miRNAs are commonly low in abundance in body fluids and exhibit a high degree of sequence homology. Kim *et al.*<sup>139</sup> developed a SERS system utilizing 3D plasmonic nanostructures for detecting miRNAs in urine. Gold nanopillars and self-assembled DNA probe-conjugated gold nanoparticles (SAP-AuNPs) were employed

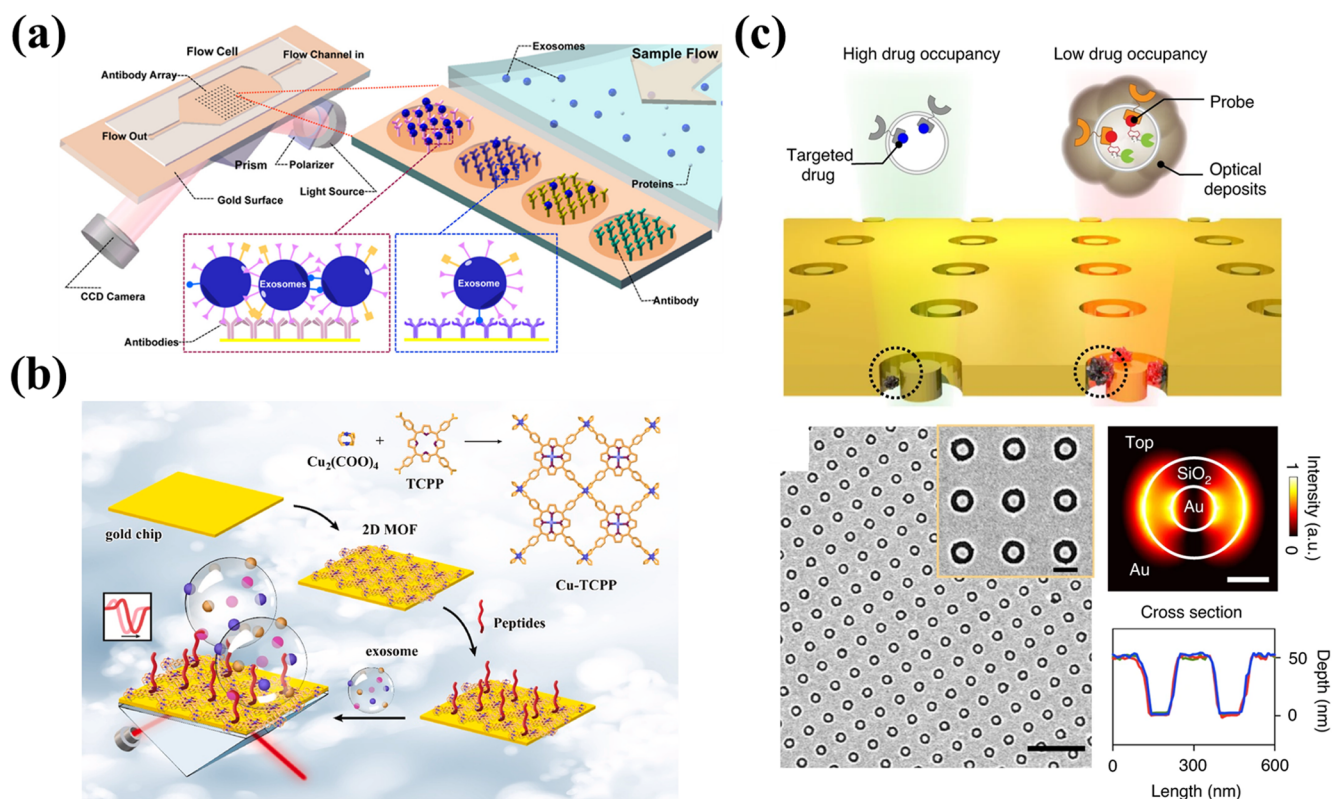


**FIG. 7.** Detection of EVs by surface plasmon resonance techniques. (a) Detection platform for EVs in cell culture supernatant combined with antibody microarray and SPR.<sup>129</sup> Reproduced from Zhu *et al.*, *Anal. Chem.* **86**, 8857–8864 (2014). (b) Schematic of SPR sensor based on 2D MOF structure.<sup>132</sup> Reproduced from Wang *et al.*, *Biosens. Bioelectron.* **201**, 113954 (2022). (c) ExoSCOPE detection platform with nanoring structure.<sup>134</sup> Reproduced from Pan *et al.*, *Nat. Nanotechnol.* **16**, 734–742 (2021).

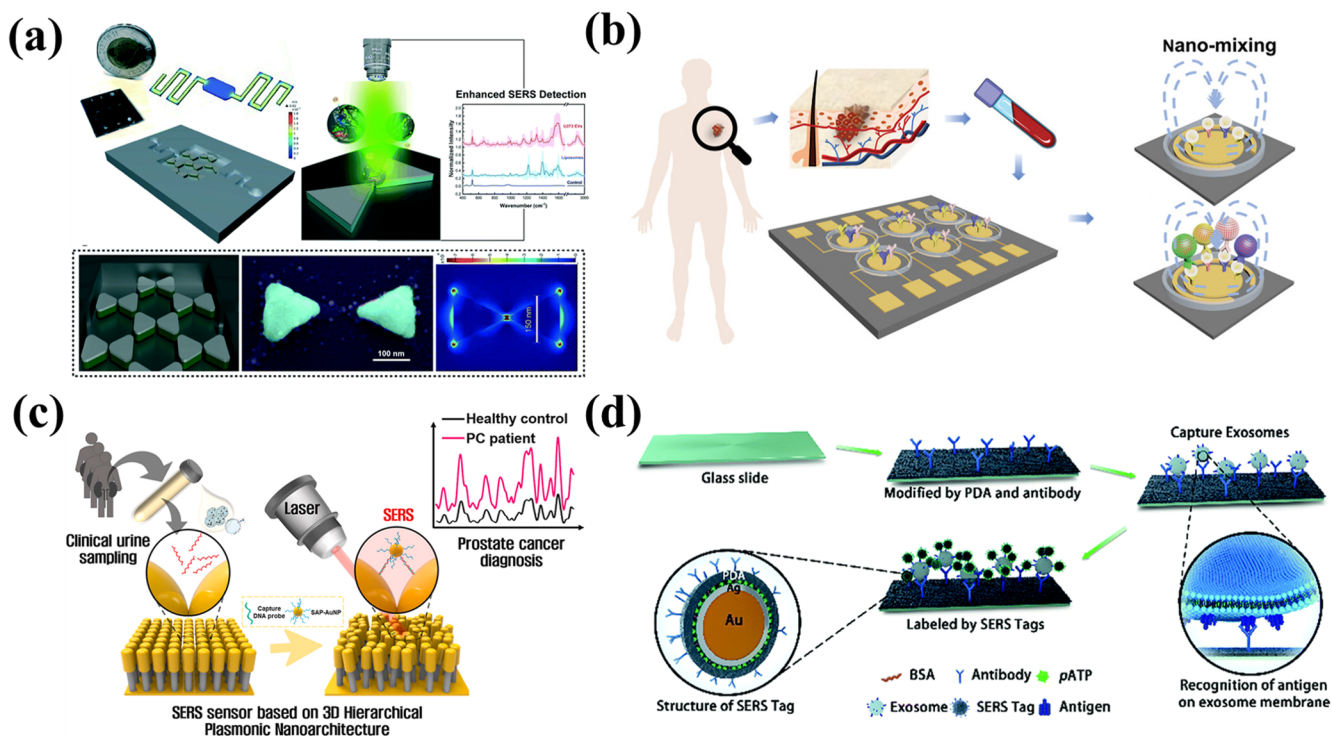


**FIG. 8.** Detection of EVs by surface-enhanced Raman scattering (SERS) techniques. (a) Microfluidic platform with butterfly-shaped structure.<sup>137</sup> Reproduced from Jalali *et al.*, *Lab Chip* **21**, 855–866 (2021). (b) EPAC-II platform combining microfluidic chip and multiplex SERS detection.<sup>138</sup> Reproduced from Wang *et al.*, *Adv. Funct. Mater.* **32**, 2010296 (2022). (c) SERS system for detecting miRNA in urine.<sup>139</sup> Reproduced from Kim *et al.*, *Biosens. Bioelectron.* **205**, 2010296 (2022). (d) SERS detection of EVs captured in a microfluidic channel.<sup>140</sup> Reproduced from Li *et al.*, *Chem. Sci.* **9**, 5372–5382 (2018).

to construct a 3D nano hierarchical structure that significantly boosted the SERS signal of miRNAs present in urine. This hierarchical plasmonic nanostructure served to extend the plasmonic hotspot between SAP-AuNPs and nanopillars, thereby increasing sensor sensitivity and enhancing clinical applicability. When the target miRNA was present, it was confined within a 3D plasmonic hotspot formed between a nanopillar head and an AuNP bearing a semi-complementary DNA probe. The sensor exhibited an exemplary detection performance, with a detection limit as low as 10 aM and a linear detection range from 10 aM to 100 nM for miRNAs (miR-10a and miR-21) in EVs of prostate cancer, surpassing that of qRT-PCR [Fig. 8(c)].

A traditional technique for EV detection involves modifying specific antibodies in microchannels. Li *et al.*<sup>140</sup> developed a pioneering SERS nanotag for sensitive EV detection utilizing a polydopamine-coated antibody–reporter–Ag(layer)–Au(core) multilayer structure. By injecting EVs derived from pancreatic cancer into the flow channel along with antibody to the macrophage migration inhibitory factor (MIF), a high-intensity SERS signal was achieved. Remarkably, only 2  $\mu$ l of clinical serum samples were required to differentiate pancreatic cancer patients from healthy individuals [Fig. 8(d)]. Inspired by honeycombs, Dong *et al.*<sup>141</sup> developed a 3D gold-coated titania microporous inverse opal (MIO) structure exhibiting remarkable EV-enhanced SERS signal performance. The MIO could directly separate and detect EVs from cancer

patients' plasma. This method has the potential for swift and label-free diagnosis of cancer by tracking the protein phosphorylation process in EVs.

#### D. Nanostructure-enabled electrochemical detection

Electrochemical detection analyzes changes in the electrical signals of target EVs and has the advantages that it is highly sensitive and low in cost, requiring only simple equipment and small samples. Typically, electrochemical detection amplifies the electrical signal of the targeted molecule through aptamer or antibody binding.<sup>142,143</sup> Zhou *et al.*<sup>144</sup> developed an aptamer-based CD63-specific EV electrochemical biosensor to quantitatively measure EVs in cell supernatants. They integrated CD63 aptamers and modified gold electrodes into a microfluidics chip and applied a methylene blue label to the aptamers via DNA probing strands. After the CD63 aptamer was hybridized into a DNA duplex, displacement of the antisense strand led to a weakened electrochemical signal without the need for antibody labeling or fluorescent image acquisition [Fig. 8(a)]. Li and co-workers<sup>145</sup> proposed a label-free EV sensor that utilized the characteristics of antibody and aptamer binding to amplify the electrochemical signal. The sensor used CD63 antibody-modified gold electrodes and specific aptamers for binding gastric cancer EVs. The addition of a heme/G-quadruplex system with rolling circle amplification (RCA) allowed for sensitive and selec-

tive detection of EVs in gastric cancer. Exposure of gastric cancer EVs to RCA stimulated abundant production of G-quadruplexes. After incubation of the reaction product with heme, the resulting heme/G-quadruplex structure catalyzed the reduction of  $H_2O_2$ , with the consequent generation of electrochemical signals. Dong *et al.*<sup>146</sup> utilized a similar strategy in which aptamer-modified magnetic beads were used to bind EVs from tumor cells. Messenger DNA (mDNA) released by these EVs then hybridized with probe DNA immobilized on gold electrodes, generating an electrochemical signal.

The use of nanostructures for electrochemical detection of EVs is a novel technique. Mathew *et al.*<sup>147</sup> developed a microfluidic electrochemical detection system that integrated nano-interdigitated electrodes, utilizing both a redox cycle and enzymatic amplification to augment electrochemical signals. The sensor comprised two sets of interdigitated nanoelectrode arrays with nanometer-scale spacing, which improved the signal amplification capability of the redox cycle. The method used an anti-EpCAM antibody on the electrode surface to capture EVs, together with a reporter anti-EpCAM antibody conjugated to alkaline phosphatase (ALP) via biotin-SAV interactions. Subsequently, captured EVs were selected sequentially twice. Reaction of the ALP with a *p*-aminophenyl phosphate substrate provided a first electrochemical signal amplification, which was followed by a second amplification due to redox cycling of the product of this reaction. This approach was successful in analyzing different concentrations of prostate cancer cells [Fig. 9(b)]. Jung's

group<sup>148</sup> introduced a detachable aptamer-based electrochemical sensor, known as the DeMEA chip. They prepared a composite of chitosan, graphene nanosheets, and  $MoS_2$  nanosheets. This composite material enhanced electrode conductivity and improved the EV capture rate owing to the increased surface area. The sensor was modified with an EpCAM aptamer and utilized a minute sample size of only 10  $\mu$ l for detection purposes.

### E. Nanostructure-enabled piezoelectric biosensor detection

Advances in acoustic technology have provided opportunities for the development of novel detection strategies based on piezoelectric biosensors and the fact that the frequencies of acoustic waves change in response to fluctuations in the propagation medium. Acoustic techniques that generate acoustic pressure and streaming effects in fluids have the advantage of good biocompatibility. Piezoelectric biosensors enable capture of extracellular vesicles (EVs), as well as functioning as tools for processing EVs (e.g., lysing EVs).<sup>149</sup> Wang *et al.*<sup>150</sup> developed a surface acoustic wave (SAW) sensor based on the use of gold nanoparticles as signal enhancers for the highly sensitive detection of EVs in blood samples obtained from cancer patients. After pre-treating the sensor, they modified its surface with an anti-CD63 antibody to immobilize EVs. Streptavidin-modified AuNPs and biotin-conjugated anti-EpCAM antibodies were then utilized to bind and recognize EVs. The SAW phase shift caused by the introduction of the AuNPs amplified the

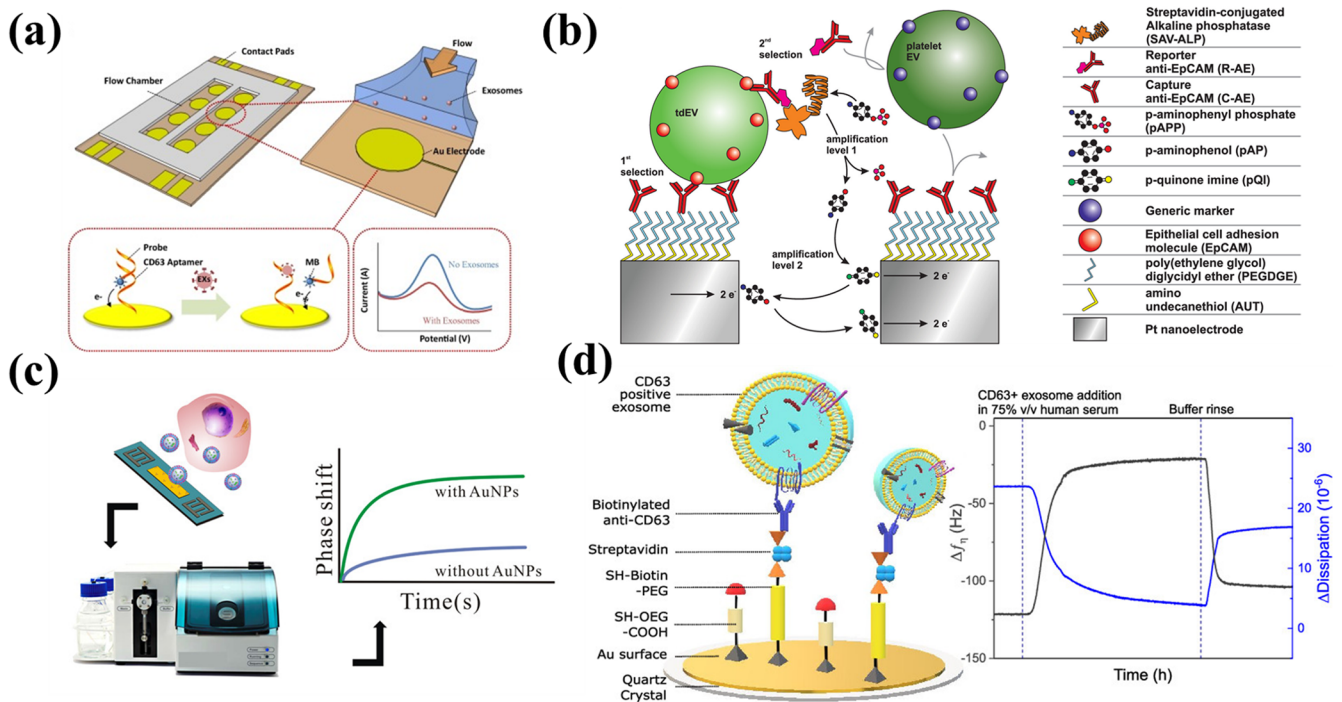


**FIG. 9.** Platforms for detecting EVs based on nanostructures. (a) Electrochemical detection platform with modified aptamers on the electrode surface.<sup>144</sup> Reproduced from Zhou *et al.*, *Methods* **97**, 88–93 (2016). (b) Electrochemical method for the detection of tumor-derived EVs using nano-interdigitated electrodes.<sup>147</sup> Reproduced from Mathew *et al.*, *Nano. Lett.* **20**, 820–828 (2020). (c) SAW sensor with gold nanoparticles as signal amplification materials.<sup>150</sup> Reproduced from Wang *et al.*, *ACS Sensors* **5**, 362–369 (2020). (d) Acoustic immunodetection of EVs with QCM-D.<sup>152</sup> Reproduced from Suthar *et al.*, *Anal. Chem.* **92**, 4082–4093 (2020).



signal, giving this sensor an improved detection sensitivity (through the mass effect). Testing demonstrated that this sensor was able to detect EVs in blood samples within 30 min [Fig. 9(c)].

Conventional methods for EV nucleic acid examination suffer from laborious operation, excessive time consumption, and limited sample retrieval rates.<sup>151</sup> Suthar *et al.*<sup>152</sup> developed a bulk acoustic wave (BAW) resonator-based sensor for EVs that employed a quartz crystal microbalance with dissipation detection (QCM-D) for label-free capture and analysis of CD63-positive EVs. An affinity-based method was used to functionalize the sensor surface with anti-CD63 antibodies. Selective separation of EVs was achieved by tracking changes in sensor resonance frequency (which depended on surface antigen species, mass, and viscoelasticity) when analytes were adsorbed onto the sensor surface. Following binding of EVs expressing CD63 to the sensor surface, the resonance frequency underwent specific changes that correlated with the physical properties and concentration of the EVs. By utilizing dissipation monitoring and frequency, this technique enabled direct evaluation of EVs at their native concentrations in complex biological samples [Fig. 9(d)].

### F. Nanostructure-enabled EV analysis at the level of individual particles

The majority of the available techniques mentioned above focus on analyzing bulk EVs rather than individual particles. However,

EVs show pronounced heterogeneity in their sources, compositions, and functions. Therefore, analyzing individual EVs is essential to unveil their diversity and complexity. In-depth analysis of single EVs can provide crucial insights into their biological roles, inter-cellular communication, and potential as diagnostic and therapeutic tools.<sup>153</sup> Moreover, single-EV analysis is a more effective strategy than bulk analysis in determining specific molecular and phenotypic features of cancer.<sup>154</sup> Consequently, innovative methods that enable precise and comprehensive single-EV analysis are in great demand.

Research on single EVs also focuses on their proteins, nucleic acids, and physical and chemical properties, similar to studies on EV populations. However, examining single EVs presents technical challenges that differ from those encountered when dealing with EV populations. The minute size of EVs (30–150 nm) and their low abundance in body fluids necessitate specialized techniques for single-EV detection and trapping. Additionally, the limited cargo of a few molecules per marker poses a challenge for signal amplification and detection.<sup>155</sup> Microfluidic techniques based on nanostructures have demonstrated significant advantages in separating and detecting single EVs. On the one hand, nanostructures can provide tiny channels and pores with similar sizes to EVs, thus enabling the separation and capture of a single EV. On the other hand, nanostructures provide superior optical detection capabilities for digital-based techniques.<sup>156</sup>

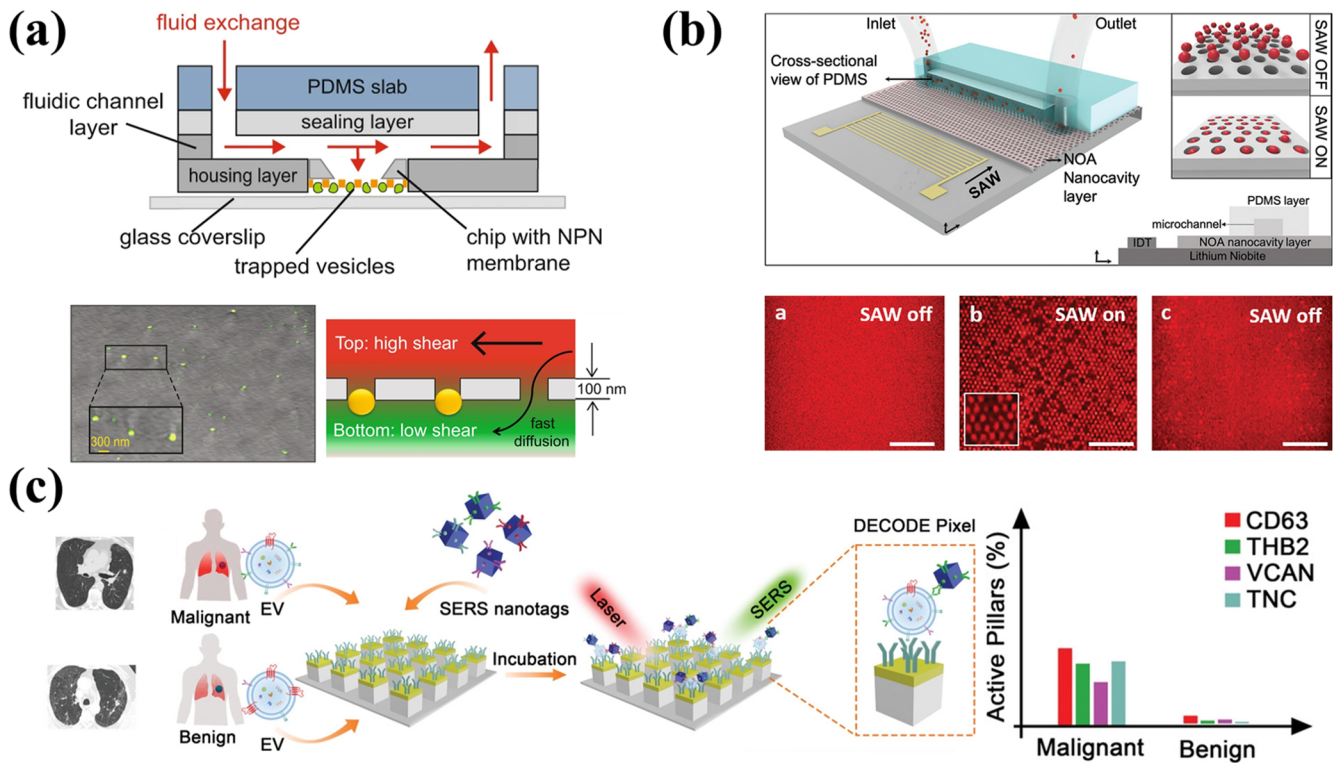


**FIG. 10.** Platforms for EV analysis at the level of individual particles based on nanostructures. (a) NPN membrane-based platform for investigation of EV properties in real time.<sup>158</sup> Reproduced from Riazanski *et al.*, *Commun. Biol.* **5**, 13 (2022). (b) Acoustic nanocavity trapping concept and result.<sup>160</sup> Reproduced from Tayebi *et al.*, *Small* **16**, 2000462 (2020). (c) Digital single-EV counting detection (DECODE) chip to differentiate malignant and benign lungs nodules.<sup>162</sup> Reproduced from Li *et al.*, *Adv. Sci.* **10**, 2000462 (2023).

Capturing and separating single EVs is a prerequisite for their analysis.<sup>157</sup> Techniques based on nanostructures and microfluidics can be divided into two categories: those based on physical properties and those based on immune affinity. Physical characteristic-based techniques generally employ nanoscale structures directly. Nelson's group<sup>158</sup> developed a novel approach to allow visualization and ion-sensitive dye measurement of single EVs [Fig. 10(a)]. A filtration-based platform was used to capture and stabilize EVs based on their size. After selective capture of secreted EVs within the pores of ultrathin nanoporous silicon nitride (NPN) membranes based on their size, real-time fluorescence imaging was used to measure the kinetics of pH changes in single vesicles brought about by the activity of the Na/H antiporter. This study has provided a new platform for studying possible mechanisms for cargo loading and maintenance at the single-EV level. In addition to single-size nanostructures, a combination of multiple-size nanostructures enabled the preparation of subpopulations of EVs in three different size fractions and an analysis of the presence of HER2 and PSMA in breast and prostate cancer cell-derived EVs, respectively, at the single-EV level.<sup>159</sup> Along with passive fluid interaction, active techniques have also been utilized to capture single EVs.<sup>160</sup> Nanostructures triggered by acoustic waves generate robust nanoscale force gradients for the trapping of single EVs [Fig. 10(b)]. A structured elastic layer placed between a microfluidic channel and a traveling SAW device provided submicrometer acoustic traps capable of capturing individual submicrometer particles. The acoustically driven deformation of the nanocavities produced time-averaged acoustic fields that directed suspended particles toward the nanocavities and trapped them there. SAWs permit massively multiplexed particle manipulation with deterministic patterning at the single-particle level.

Immune-affinity traps capture EVs by binding a selected membrane protein to its corresponding antibody immobilized on a nanostructure.<sup>161</sup> The small size of the nanostructure and an appropriate optical enhancement effect then enable a lower detection limit to be reached.<sup>130</sup> Trau and co-workers<sup>162</sup> introduced the DECODE chip, which captured EVs on a nanostructured pillar chip, confined individual EVs, and used SERS to detect three lung cancer-associated biomarkers as well as a generic single-EV biomarker [Fig. 10(c)]. The DECODE chip was used to generate digitally acquired single-EV molecular profiles in a cohort of 33 subjects including both those with malignant and benign lung nodules, as well as healthy individuals. DECODE was able to provide specific molecular profiles for single EVs that enabled differentiation between malignant and benign nodules with an area under the curve (AUC) of 0.85.

Single-EV analysis utilizing nanostructures presents several advantages over traditional bulk analysis methods. By analyzing EVs individually, researchers can obtain more detailed information about their characteristics and better understand the relationship between different subtypes of vesicular molecules and diseases. The high-precision counting and improved detection limits provided by nanostructure-based methods can also help detect disease biomarkers with greater accuracy, potentially leading to earlier and more accurate diagnoses. Additionally, these methods may be useful for monitoring disease progression and treatment response. While current nanostructure-based methods may be cumbersome and have low throughput, ongoing research is focused on developing more efficient and scalable techniques. As these methods continue to

improve, they hold promise as valuable diagnostic tools for cancer and other diseases.

#### IV. CONCLUSION AND OUTLOOK

As essential biomarkers in liquid biopsies, EVs have shown significant potential in clinical diagnosis. Much work has been done on the separation and detection of these complex nanoscale particles and the detailed biological information that they encapsulate. This review commenced by outlining the constituents and biogenesis of EVs, and the traditional methods used for their separation and detection. This was followed by a summary of the latest advances in nanostructure-based procedures for EV separation and detection, as well as their application in bioanalysis and disease diagnosis. Thanks to advances in nanofabrication technology, novel techniques based on nanostructures are able to handle complex bodily fluid samples and provide extensive insights into the function and structure of EVs. Nevertheless, these nanostructure-based techniques are still in their early stages of development.

1. Owing to the inherently small sample volume of microfluidics in nanostructures, the resulting separation throughput is very low (of the order of just microliters per minute), which falls far below the liter per minute requirement of clinical applications. Nonetheless, even such low sample sizes and throughputs have minimal impact on detection results. Furthermore, EVs in samples (especially bodily fluids) are biologically heterogeneous, with a mixture of multiple subtypes of EVs. Thus, the combined implementation of several separation techniques will be needed to achieve high-resolution separation. However, separating EVs of pathological cells from those of normal cells poses a challenge. Moreover, employing passive or active methods that combine acoustic and electric fields during EV separation inevitably results in EV damage. Amplified electric and acoustic fields can produce thermal effects, which irreversibly affect the biological activity of EVs. Overcoming these limitations will enable a deeper appreciation to be achieved of the roles of different EV subsets in early-stage cancer and in disease prognosis, allowing for personalized therapy development.
2. Regarding detection, conventional methods often necessitate an all-inclusive EV characterization through NTA, western blotting, SEM, and qRT-PCR. Contemporary studies require greater EV purity. The integration of nanostructures and optical detection significantly reduces the detection limits, enabling more precise and sensitive EV detection. Different research groups utilize different antibodies or aptamers for cancer diagnoses, and hence have varying views on analysis and characterization techniques. Thus, there is a pressing demand to establish standardized EV detection processes.
3. Integrating nanostructures with microfluidic technology in the biomedical domain assists in system miniaturization. The use of lab-on-chip equipment, including sample pretreatment, separation, and detection, efficiently reduces excessive processing periods, exorbitant costs, and laborious clinical sample management. Physicians have acknowledged the advances that can be achieved through the use of EV-based point-of-care (POC) devices. Also, notably, machine-learning



algorithms and other artificial intelligence techniques can provide novel approaches for high-dimensional EV data processing and analysis. Such algorithms should enable enhanced cancer detection, diagnosis, and classification, boosting the potential for clinical application of multifunctional POC devices.

## ACKNOWLEDGMENTS

The authors gratefully acknowledge financial support from the National Key R&D Program of China (Grant No. 2018YFE0118700), the National Natural Science Foundation of China (NSFC Grant No. 62174119), the 111 Project (No. B07014), and the Foundation for Talent Scientists of Nanchang Institute for Micro-technology of Tianjin University.

## AUTHOR DECLARATIONS

### Conflict of Interest

The authors have no conflicts to disclose.

## DATA AVAILABILITY

Data sharing is not applicable to this article as no new data were created or analyzed in this study.

## REFERENCES

- Lobb RJ, Becker M, Wen Wen S, et al. Optimized exosome isolation protocol for cell culture supernatant and human plasma. *J Extracell Vesicles* 2015;4(1):27031. <https://doi.org/10.3402/jev.v4.27031>.
- Gibbins DJ, Ciaudo C, Erhardt M, Voinnet O. Multivesicular bodies associate with components of miRNA effector complexes and modulate miRNA activity. *Nat Cell Biol* 2009;11(9):1143–1149. <https://doi.org/10.1038/ncb1929>.
- Yuan K, Shamskhov EA, Orcholski ME, et al. Loss of endothelium-derived Wnt5a is associated with reduced pericyte recruitment and small vessel loss in pulmonary arterial hypertension. *Circulation* 2019;139(14):1710–1724. <https://doi.org/10.1161/circulationaha.118.037642>.
- György B, Módos K, Pállinger É, et al. Detection and isolation of cell-derived microparticles are compromised by protein complexes resulting from shared biophysical parameters. *Blood* 2011;117(4):e39–e48. <https://doi.org/10.1182/blood-2010-09-307595>.
- Raposo G, Stoorvogel W. Extracellular vesicles: Exosomes, microvesicles, and friends. *J Cell Biol* 2013;200(4):373–383. <https://doi.org/10.1083/jcb.201211138>.
- Properzi F, Logozzi M, Fais S. Exosomes: The future of biomarkers in medicine. *Biomarkers Med* 2013;7(5):769–778. <https://doi.org/10.2217/bmm.13.63>.
- Chen G, Huang AC, Zhang W, et al. Exosomal PD-L1 contributes to immunosuppression and is associated with anti-PD-1 response. *Nature* 2018;560(7718):382–386. <https://doi.org/10.1038/s41586-018-0392-8>.
- Gardiner C, D. D. Vizio, Sahoo S, et al. Techniques used for the isolation and characterization of extracellular vesicles: Results of a worldwide survey. *J Extracell Vesicles* 2016;5(1):32945. <https://doi.org/10.3402/jev.v5.32945>.
- Samuel M, Chisanga D, Liem M, et al. Bovine milk-derived exosomes from colostrum are enriched with proteins implicated in immune response and growth. *Sci Rep* 2017;7(1):5933. <https://doi.org/10.1038/s41598-017-06288-8>.
- Shirejini SZ, Inci F. The Yin and Yang of exosome isolation methods: Conventional practice, microfluidics, and commercial kits. *Biotechnol Adv* 2022;54:107814. <https://doi.org/10.1016/j.biotechadv.2021.107814>.
- Jenjaroenpun P, Kremenska Y, Nair VM, Kremenskoy M, Joseph B, Kurochkin IV. Characterization of RNA in exosomes secreted by human breast cancer cell lines using next-generation sequencing. *PeerJ* 2013;1:e201. <https://doi.org/10.7717/peerj.201>.
- Théry C, Zitvogel L, Amigorena S. Exosomes: Composition, biogenesis and function. *Nat Rev Immunol* 2002;2(8):569–579. <https://doi.org/10.1038/nri855>.
- Nabet BY, Qiu Y, Shabason JE, et al. Exosome RNA unshielding couples stromal activation to pattern recognition receptor signaling in cancer. *Cell* 2017;170(2):352–366.e13. <https://doi.org/10.1016/j.cell.2017.06.031>.
- Liang LG, Kong MQ, Zhou S, et al. An integrated double-filtration microfluidic device for isolation, enrichment and quantification of urinary extracellular vesicles for detection of bladder cancer. *Sci Rep* 2017;7(1):46224. <https://doi.org/10.1038/srep46224>.
- Szczepanski MJ, Szajnik M, Welsh A, Whiteside TL, Boyiadzis M. Blast-derived microvesicles in sera from patients with acute myeloid leukemia suppress natural killer cell function via membrane-associated transforming growth factor-β1. *Haematologica* 2011;96(9):1302–1309. <https://doi.org/10.3324/haematol.2010.039743>.
- Whiteside TL. Tumor-derived exosomes and their role in cancer progression. in *Advances in Clinical Chemistry*, edited by Makowski GS. Elsevier. 2016. Vol. 74. pp. 103–141.
- Zhan Y, Du L, Wang L, et al. Expression signatures of exosomal long non-coding RNAs in urine serve as novel non-invasive biomarkers for diagnosis and recurrence prediction of bladder cancer. *Mol Cancer* 2018;17(1):142. <https://doi.org/10.1186/s12943-018-0893-y>.
- Li C, Lv Y, Shao C, et al. Tumor-derived exosomal lncRNA GAS5 as a biomarker for early-stage non-small-cell lung cancer diagnosis. *J Cell Physiol* 2019;234(11):20721–20727. <https://doi.org/10.1002/jcp.28678>.
- Wang J, Ma P, Kim DH, Liu BF, Demirci U. Towards microfluidic-based exosome isolation and detection for tumor therapy. *Nano Today* 2021;37:101066. <https://doi.org/10.1016/j.nantod.2020.101066>.
- Chiriaco MS, Bianco M, Nigro A, et al. Lab-on-Chip for exosomes and microvesicles detection and characterization. *Sensors* 2018;18(10):3175. <https://doi.org/10.3390/s18103175>.
- Dash S, Wu CC, Wu CC, et al. Extracellular vesicle membrane protein profiling and targeted mass spectrometry unveil CD59 and tetraspanin 9 as novel plasma biomarkers for detection of colorectal cancer. *Cancers* 2022;15(1):177. <https://doi.org/10.3390/cancers15010177>.
- Li P, Xu Z, Liu T, et al. Circular RNA sequencing reveals serum exosome circular RNA panel for high-grade astrocytoma diagnosis. *Clin Chem* 2022;68(2):332–343. <https://doi.org/10.1093/clinchem/hvab254>.
- Liang G, Zhu Y, Ali DJ, et al. Engineered exosomes for targeted co-delivery of miR-21 inhibitor and chemotherapeutics to reverse drug resistance in colon cancer. *J Nanobiotechnol* 2020;18(1):10. <https://doi.org/10.1186/s12951-019-0563-2>.
- Hassanpour Tamrin S, Sanati Nezhad A, Sen A. Label-free isolation of exosomes using microfluidic technologies. *ACS Nano* 2021;15(11):17047–17079. <https://doi.org/10.1021/acsnano.1c03469>.
- Li P, Kaslan M, Lee SH, Yao J, Gao Z. Progress in exosome isolation techniques. *Theranostics* 2017;7(3):789–804. <https://doi.org/10.7150/thno.18133>.
- Patel GK, Khan MA, Zubair H, et al. Comparative analysis of exosome isolation methods using culture supernatant for optimum yield, purity and downstream applications. *Sci Rep* 2019;9(1):5335. <https://doi.org/10.1038/s41598-019-41800-2>.
- Gandham S, Su X, Wood J, et al. Technologies and standardization in research on extracellular vesicles. *Trends Biotechnol* 2020;38(10):1066–1098. <https://doi.org/10.1016/j.tibtech.2020.05.012>.
- Fekete S, Beck A, Veuthey JL, Guillaume D. Theory and practice of size exclusion chromatography for the analysis of protein aggregates. *J Pharm Biomed Anal* 2014;101:161–173. <https://doi.org/10.1016/j.jpba.2014.04.011>.
- Blans K, Hansen MS, Sørensen LV, et al. Pellet-free isolation of human and bovine milk extracellular vesicles by size-exclusion chromatography. *J Extracell Vesicles* 2017;6(1):1294340. <https://doi.org/10.1080/20013078.2017.1294340>.
- Sódar BW, Kittel Á, Pálóczi K, et al. Low-density lipoprotein mimics blood plasma-derived exosomes and microvesicles during isolation and detection. *Sci Rep* 2016;6(1):24316. <https://doi.org/10.1038/srep24316>.
- Tengattini S. Chromatographic approaches for purification and analytical characterization of extracellular vesicles: Recent advancements. *Chromatographia* 2019;82(1):415–424. <https://doi.org/10.1007/s10337-018-3637-7>.

- <sup>32</sup> Yamamoto KR, Alberts BM, Benzinger R, Lawhorne L, Treiber G. Rapid bacteriophage sedimentation in the presence of polyethylene glycol and its application to large-scale virus purification. *Virology* 1970;40(3):734–744. [https://doi.org/10.1016/0042-6822\(70\)90218-7](https://doi.org/10.1016/0042-6822(70)90218-7).
- <sup>33</sup> Kim D, Nishida H, An SY, Shetty AK, Bartosh TJ, Prockop DJ. Chromatographically isolated CD63<sup>+</sup> CD81<sup>+</sup> extracellular vesicles from mesenchymal stromal cells rescue cognitive impairments after TBI. *Proc Natl Acad Sci USA* 2016;113(1):170–175. <https://doi.org/10.1073/pnas.1522297113>.
- <sup>34</sup> Zeringer E, Barta T, Li M, Vlassov AV. Strategies for isolation of exosomes. *Cold Spring Harb Protoc*;2015(4):319. <https://doi.org/10.1101/pdb.top074476>.
- <sup>35</sup> Batrakova E V, Kim MS. Using exosomes, naturally-equipped nanocarriers, for drug delivery. *J Controlled Release* 2015;219:396–405. <https://doi.org/10.1016/j.jconrel.2015.07.030>.
- <sup>36</sup> Zarovni N, Corrado A, Guazzi P, et al. Integrated isolation and quantitative analysis of exosome shuttled proteins and nucleic acids using immunocapture approaches. *Methods* 2015;87:46–58. <https://doi.org/10.1016/j.ymeth.2015.05.028>.
- <sup>37</sup> Gurunathan S, Kang MH, Jeyaraj M, Qasim M, Kim JH. Review of the isolation, characterization, biological function, and multifarious therapeutic approaches of exosomes. *Cells* 2019;8(4):307. <https://doi.org/10.3390/cells8040307>.
- <sup>38</sup> Wang Z, Wu H, Fine D, et al. Ciliated micropillars for the microfluidic-based isolation of nanoscale lipid vesicles. *Lab Chip* 2013;13(15):2879–2882. <https://doi.org/10.1039/c3lc41343h>.
- <sup>39</sup> Alvarez ML, Khosroheidari M, Kanchi Ravi R, DiStefano JK. Comparison of protein, microRNA, and mRNA yields using different methods of urinary exosome isolation for the discovery of kidney disease biomarkers. *Kidney Int* 2012;82(9):1024–1032. <https://doi.org/10.1038/ki.2012.256>.
- <sup>40</sup> Greening DW, Xu R, Ji H, Tauro BJ, Simpson RJ. A protocol for exosome isolation and characterization: Evaluation of ultracentrifugation, density-gradient separation, and immunoaffinity capture methods. in *Proteomic Profiling: Methods and Protocols*, edited by Posch A. Springer. New York. 2015. pp. 179–209.
- <sup>41</sup> Vergauwen G, Dhondt B, Van Deun J, et al. Confounding factors of ultrafiltration and protein analysis in extracellular vesicle research. *Sci Rep* 2017;7(1):2704. <https://doi.org/10.1038/s41598-017-02599-y>.
- <sup>42</sup> Koliha N, Wiencek Y, Heider U, et al. A novel multiplex bead-based platform highlights the diversity of extracellular vesicles. *J Extracell Vesicles* 2016;5(1):29975. <https://doi.org/10.3402/jev.v5.29975>.
- <sup>43</sup> Li F, You M, Li S, et al. Paper-based point-of-care immunoassays: Recent advances and emerging trends. *Biotechnol Adv* 2020;39:107442. <https://doi.org/10.1016/j.biotechadv.2019.107442>.
- <sup>44</sup> Li B, Zang G, Zhong W, et al. Activation of CD137 signaling promotes neointimal formation by attenuating TET2 and transferring from endothelial cell-derived exosomes to vascular smooth muscle cells. *Biomed Pharmacother* 2020;121:109593. <https://doi.org/10.1016/j.biopha.2019.109593>.
- <sup>45</sup> Cutler P. Immunoaffinity chromatography. in *Protein Purification Protocols*, edited by Cutler P. Humana Press. 2004. pp. 167–177.
- <sup>46</sup> Tauro BJ, Greening DW, Mathias RA, et al. Comparison of ultracentrifugation, density gradient separation, and immunoaffinity capture methods for isolating human colon cancer cell line LIM1863-derived exosomes. *Methods* 2012;56(2):293–304. <https://doi.org/10.1016/j.ymeth.2012.01.002>.
- <sup>47</sup> Soo CY, Song Y, Zheng Y, et al. Nanoparticle tracking analysis monitors microvesicle and exosome secretion from immune cells. *Immunology* 2012;136(2):192–197. <https://doi.org/10.1111/j.1365-2567.2012.03569.x>.
- <sup>48</sup> Hoo CM, Starostin N, West P, Mecartney ML. A comparison of atomic force microscopy (AFM) and dynamic light scattering (DLS) methods to characterize nanoparticle size distributions. *J Nanopart Res* 2008;10(S1):89–96. <https://doi.org/10.1007/s11051-008-9435-7>.
- <sup>49</sup> Erdbrügger U, Lannigan J. Analytical challenges of extracellular vesicle detection: A comparison of different techniques. *Cytometry Part A* 2016;89(2):123–134. <https://doi.org/10.1002/cyto.a.22795>.
- <sup>50</sup> Khan S, Bennit HF, Turay D, et al. Early diagnostic value of survivin and its alternative splice variants in breast cancer. *BMC Cancer* 2014;14(1):176. <https://doi.org/10.1186/1471-2407-14-176>.
- <sup>51</sup> Fan Z, Yu J, Lin J, Liu Y, Liao Y. Exosome-specific tumor diagnosis via biomedical analysis of exosome-containing microRNA biomarkers. *Analyst* 2019;144(19):5856–5865. <https://doi.org/10.1039/c9an00777f>.
- <sup>52</sup> Sina AAI, Vaidyanathan R, Wuethrich A, Carrascosa LG, Trau M. Label-free detection of exosomes using a surface plasmon resonance biosensor. *Anal Bioanal Chem* 2019;411(7):1311–1318. <https://doi.org/10.1007/s00216-019-01608-5>.
- <sup>53</sup> Vogel R, Willmott G, Kozak D, et al. Quantitative sizing of nano/microparticles with a tunable elastomeric pore sensor. *Anal Chem* 2011;83(9):3499–3506. <https://doi.org/10.1021/ac200195n>.
- <sup>54</sup> Dey S, Trau M, Koo KM. Surface-enhanced Raman spectroscopy for cancer immunotherapy applications: Opportunities, challenges, and current progress in nanomaterial strategies. *Nanomaterials* 2020;10(6):1145. <https://doi.org/10.3390/nano10061145>.
- <sup>55</sup> Tzaridis T, Bachurski D, Liu S, et al. Extracellular vesicle separation techniques impact results from human blood samples: Considerations for diagnostic applications. *Int J Mol Sci* 2021;22(17):9211. <https://doi.org/10.3390/ijms22179211>.
- <sup>56</sup> Mahgoub EO, Razmara E, Bitaraf A, et al. Advances of exosome isolation techniques in lung cancer. *Mol Biol Rep* 2020;47(9):7229–7251. <https://doi.org/10.1007/s11033-020-05715-w>.
- <sup>57</sup> Yang D, Zhang W, Zhang H, et al. Progress, opportunity, and perspective on exosome isolation - efforts for efficient exosome-based theranostics. *Theranostics* 2020;10(8):3684–3707. <https://doi.org/10.7150/thno.41580>.
- <sup>58</sup> Le MCN, Fan HZ. Exosome isolation using nanostructures and microfluidic devices. *Biomed Mater* 2021;16(2):22005. <https://doi.org/10.1088/1748-605x/abde70>.
- <sup>59</sup> Talebjedi B, Tasnim N, Hoorfar M, Mastromonaco GF, De Almeida Monteiro Melo Ferraz M. Exploiting microfluidics for extracellular vesicle isolation and characterization: Potential use for standardized embryo quality assessment. *Front Vet Sci* 2021;7:620809. <https://doi.org/10.3389/fvets.2020.620809>.
- <sup>60</sup> Iliescu FS, Vrtačnik D, Neuzil P, Iliescu C. Microfluidic technology for clinical applications of exosomes. *Micromachines* 2019;10(6):392. <https://doi.org/10.3390/mi10060392>.
- <sup>61</sup> Voldman J. Electrical forces for microscale cell manipulation. *Annu Rev Biomed Eng* 2006;8(1):425–454. <https://doi.org/10.1146/annurev.bioeng.8.061505.095739>.
- <sup>62</sup> Kirschner AY, Cheng YH, Paul DR, Field RW, Freeman BD. Fouling mechanisms in constant flux crossflow ultrafiltration. *J Membr Sci* 2019;574:65–75. <https://doi.org/10.1016/j.memsci.2018.12.001>.
- <sup>63</sup> Liu F, Vermesh O, Mani V, et al. The exosome total isolation chip. *ACS Nano* 2017;11(11):10712–10723. <https://doi.org/10.1021/acsnano.7b04878>.
- <sup>64</sup> Dong X, Chi J, Zheng L, et al. Efficient isolation and sensitive quantification of extracellular vesicles based on an integrated ExoID-Chip using photonic crystals. *Lab Chip* 2019;19(17):2897–2904. <https://doi.org/10.1039/c9lc00445a>.
- <sup>65</sup> Seder I, Moon H, Kang SJ, Shin S, Rhee WJ, Kim SJ. Size-selective filtration of extracellular vesicles with a movable-layer device. *Lab Chip* 2022;22(19):3699–3707. <https://doi.org/10.1039/d2lc00411ks>.
- <sup>66</sup> Diaz-Reinoso B. Concentration and purification of seaweed extracts using membrane technologies. in *Sustainable Seaweed Technologies*, edited by Torres MD, Kraan S, Dominguez H. Elsevier. 2020. pp. 371–390.
- <sup>67</sup> Woo HK, Park J, Ku JY, et al. Urine-based liquid biopsy: Non-invasive and sensitive AR-V7 detection in urinary EVs from patients with prostate cancer. *Lab Chip* 2019;19(1):87–97. <https://doi.org/10.1039/c8lc01185k>.
- <sup>68</sup> Woo HK, Sunkara V, Park J, et al. Exodisc for rapid, size-selective, and efficient isolation and analysis of nanoscale extracellular vesicles from biological samples. *ACS Nano* 2017;11(2):1360–1370. <https://doi.org/10.1021/acsnano.6b06131>.
- <sup>69</sup> Sunkara V, Kim CJ, Park J, et al. Fully automated, label-free isolation of extracellular vesicles from whole blood for cancer diagnosis and monitoring. *Theranostics* 2019;9(7):1851–1863. <https://doi.org/10.7150/thno.32438>.
- <sup>70</sup> Han Z, Peng C, Yi J, et al. Highly efficient exosome purification from human plasma by tangential flow filtration based microfluidic chip. *Sens Actuators B* 2021;333:129563. <https://doi.org/10.1016/j.snb.2021.129563>.
- <sup>71</sup> Dehghani M, Lucas K, Flax J, McGrath J, Gaborski T. Tangential flow microfluidics for the capture and release of nanoparticles and extracellular vesicles on conventional and ultrathin membranes. *Adv Mater Technol* 2019;4(11):1900539. <https://doi.org/10.1002/admt.201900539>.
- <sup>72</sup> Rahong S, Yasui T, Yanagida T, et al. Three-dimensional nanowire structures for ultra-fast separation of DNA, protein and RNA molecules. *Sci Rep* 2015;5(1):10584. <https://doi.org/10.1038/srep10584>.

- <sup>73</sup>Barutta F, Tricarico M, Corbelli A, et al. Urinary exosomal MicroRNAs in incipient diabetic nephropathy. *PLoS One* 2013;8(11):e73798. <https://doi.org/10.1371/journal.pone.0073798>.
- <sup>74</sup>Yasui T, Yanagida T, Ito S, et al. Unveiling massive numbers of cancer-related urinary-microRNA candidates via nanowires. *Sci Adv* 2017;3(12):e1701133. <https://doi.org/10.1126/sciadv.1701133>.
- <sup>75</sup>Yeh YT, Zhou Y, Zou D, et al. Rapid size-based isolation of extracellular vesicles by three-dimensional carbon nanotube arrays. *ACS Appl Mater Interfaces* 2020;12(11):13134–13139. <https://doi.org/10.1021/acsmi.9b20990>.
- <sup>76</sup>Wunsch BH, Smith JT, Gifford SM, et al. Nanoscale lateral displacement arrays for the separation of exosomes and colloids down to 20 nm. *Nat Nanotechnol* 2016;11(11):936–940. <https://doi.org/10.1038/nnano.2016.134>.
- <sup>77</sup>Smith JT, Wunsch BH, Dogra N, et al. Integrated nanoscale deterministic lateral displacement arrays for separation of extracellular vesicles from clinically-relevant volumes of biological samples. *Lab Chip* 2018;18(24):3913–3925. <https://doi.org/10.1039/c8lc01017j>.
- <sup>78</sup>Huang LR, Cox EC, Austin RH, Sturm JC. Continuous particle separation through deterministic lateral displacement. *Science* 2004;304(5673):987–990. <https://doi.org/10.1126/science.1094567>.
- <sup>79</sup>Inglis DW, Davis JA, Austin RH, Sturm JC. Critical particle size for fractionation by deterministic lateral displacement. *Lab Chip* 2006;6(5):655–658. <https://doi.org/10.1039/b515371a>.
- <sup>80</sup>Liu Z, Huang F, Du J, et al. Rapid isolation of cancer cells using microfluidic deterministic lateral displacement structure. *Biomicrofluidics* 2013;7(1):11801. <https://doi.org/10.1063/1.4774308>.
- <sup>81</sup>Davis JA, Inglis DW, Morton KJ, et al. Deterministic hydrodynamics: Taking blood apart. *Proc Natl Acad Sci USA* 2006;103(40):14779–14784. <https://doi.org/10.1073/pnas.0605967103>.
- <sup>82</sup>Beech JP, Ho BD, Garriss G, Oliveira V, Henriques-Normark B, Tegenfeldt JO. Separation of pathogenic bacteria by chain length. *Anal Chim Acta* 2018;1000:223–231. <https://doi.org/10.1016/j.aca.2017.11.050>.
- <sup>83</sup>Santana SM, Antonyak MA, Cerione RA, Kirby BJ. Microfluidic isolation of cancer-cell-derived microvesicles from heterogeneous extracellular shed vesicle populations. *Biomed Microdev* 2014;16(6):869–877. <https://doi.org/10.1007/s10544-014-9891-z>.
- <sup>84</sup>Zeming KK, Thakor N V, Zhang Y, Chen CH. Real-time modulated nanoparticle separation with an ultra-large dynamic range. *Lab Chip* 2016;16(1):75–85. <https://doi.org/10.1039/c5lc01051a>.
- <sup>85</sup>Wunsch BH, Hsieh KY, Kim SC, et al. Advancements in throughput, lifetime, purification, and workflow for integrated nanoscale deterministic lateral displacement. *Adv Mater Technol* 2021;6(4):2001083. <https://doi.org/10.1002/admt.202001083>.
- <sup>86</sup>Wang Z, Li F, Rufo J, et al. Acoustofluidic salivary exosome isolation. *J Mol Diagn* 2020;22(1):50–59. <https://doi.org/10.1016/j.jmoldx.2019.08.004>.
- <sup>87</sup>Shi L, Rana A, Esfandiari L. A low voltage nanopipette dielectrophoretic device for rapid entrapment of nanoparticles and exosomes extracted from plasma of healthy donors. *Sci Rep* 2018;8(1):6751. <https://doi.org/10.1038/s41598-018-25026-2>.
- <sup>88</sup>Ayala-Mar S, Perez-Gonzalez VH, Mata-Gómez MA, Gallo-Villanueva RC, González-Valdez J. Electrokinetically driven exosome separation and concentration using dielectrophoretic-enhanced PDMS-based microfluidics. *Anal Chem* 2019;91(23):14975–14982. <https://doi.org/10.1021/acs.analchem.9b03448>.
- <sup>89</sup>Lenshof A, Magnusson C, Laurell T. Acoustofluidics 8: Applications of acoustophoresis in continuous flow microsystems. *Lab Chip* 2012;12(7):1210–1223. <https://doi.org/10.1039/c2lc21256k>.
- <sup>90</sup>Zhang P, Bachman H, Ozelik A, Huang TJ. Acoustic microfluidics. *Annu Rev Anal Chem* 2020;13(1):17–43. <https://doi.org/10.1146/annurev-anchem-090919-102205>.
- <sup>91</sup>Wu H, Tang Z, You R, et al. Manipulations of micro/nanoparticles using gigahertz acoustic streaming tweezers. *Nanotechnol Precis Eng* 2022;5(2):023001. <https://doi.org/10.1063/1.50009954>.
- <sup>92</sup>Wei W, Wang Y, Wang Z, Duan X. Microscale acoustic streaming for biomedical and bioanalytical applications. *TRAC Trends Anal Chem* 2023;160:116958. <https://doi.org/10.1016/j.trac.2023.116958>.
- <sup>93</sup>Wu M, Mao Z, Chen K, et al. Acoustic separation of nanoparticles in continuous flow. *Adv Funct Mater* 2017;27(14):1606039. <https://doi.org/10.1002/adfm.201606039>.
- <sup>94</sup>Chen Y, Zhu Q, Cheng L, et al. Exosome detection via the ultrafast-isolation system: EXODUS. *Nat Methods* 2021;18(2):212–218. <https://doi.org/10.1038/s41592-020-01034-x>.
- <sup>95</sup>Davies RT, Kim J, Jang SC, Choi EJ, Gho YS, Park J. Microfluidic filtration system to isolate extracellular vesicles from blood. *Lab Chip* 2012;12(24):5202–5210. <https://doi.org/10.1039/c2lc41006k>.
- <sup>96</sup>Cho S, Jo W, Heo Y, Kang JY, Kwak R, Park J. Isolation of extracellular vesicle from blood plasma using electrophoretic migration through porous membrane. *Sens Actuators B* 2016;233:289–297. <https://doi.org/10.1016/j.snb.2016.04.091>.
- <sup>97</sup>Marczak S, Richards K, Ramshani Z, et al. Simultaneous isolation and pre-concentration of exosomes by ion concentration polarization. *Electrophoresis* 2018;39(15):2029–2038. <https://doi.org/10.1002/elps.201700491>.
- <sup>98</sup>Lai YC, Keh HJ. Transient electrophoresis of a charged porous particle. *Electrophoresis* 2020;41(3–4):259–265. <https://doi.org/10.1002/elps.201900413>.
- <sup>99</sup>Edwards TD, Bevan MA. Controlling colloidal particles with electric fields. *Langmuir* 2014;30(36):10793–10803. <https://doi.org/10.1021/la500178b>.
- <sup>100</sup>Esmailsabzali H, Beischlag TV, Cox ME, Parameswaran AM, Park EJ. Detection and isolation of circulating tumor cells: Principles and methods. *Biotechnol Adv* 2013;31(7):1063–1084. <https://doi.org/10.1016/j.biotechadv.2013.08.016>.
- <sup>101</sup>Mata-Gomez MA, Perez-Gonzalez VH, Gallo-Villanueva RC, Gonzalez-Valdez J, Rito-Palmares M, Martinez-Chapa SO. Modelling of electrokinetic phenomena for capture of PEGylated ribonuclease A in a microdevice with insulating structures. *Biomicrofluidics* 2016;10(3):033106. <https://doi.org/10.1063/1.4954197>.
- <sup>102</sup>Ibsen SD, Wright J, Lewis JM, et al. Rapid isolation and detection of exosomes and associated biomarkers from plasma. *ACS Nano* 2017;11(7):6641–6651. <https://doi.org/10.1021/acsnano.7b00549>.
- <sup>103</sup>Chen Z, Yang Y, Yamaguchi H, Hung MC, Kameoka J. Isolation of cancer-derived extracellular vesicle subpopulations by a size-selective microfluidic platform. *Biomicrofluidics* 2020;14(3):34113. <https://doi.org/10.1063/5.0008438>.
- <sup>104</sup>Mogi K, Hayashida K, Yamamoto T. Damage-less handling of exosomes using an ion-depletion zone in a microchannel. *Anal Sci* 2018;34(8):875–880. <https://doi.org/10.2116/analsci.17p462>.
- <sup>105</sup>Masud MK, Na J, Younus M, et al. Superparamagnetic nanoarchitectures for disease-specific biomarker detection. *Chem Soc Rev* 2019;48(24):5717–5751. <https://doi.org/10.1039/c9cs00174c>.
- <sup>106</sup>Boriachek K, Masud MK, Palma C, et al. Avoiding pre-isolation step in exosome analysis: Direct isolation and sensitive detection of exosomes using gold-loaded nanoporous ferric oxide nanozymes. *Anal Chem* 2019;91(6):3827–3834. <https://doi.org/10.1021/acs.analchem.8b03619>.
- <sup>107</sup>Huang X, Liu Y, Yung B, Xiong Y, Chen X. Nanotechnology-enhanced no-wash biosensors for in vitro diagnostics of cancer. *ACS Nano* 2017;11(6):5238–5292. <https://doi.org/10.1021/acsnano.7b02618>.
- <sup>108</sup>Chang M, Chang YJ, Chao PY, Yu Q. Exosome purification based on PEG-coated Fe<sub>3</sub>O<sub>4</sub> nanoparticles. *PLoS One* 2018;13(6):e0199438. <https://doi.org/10.1371/journal.pone.0199438>.
- <sup>109</sup>Ko J, Bhagwat N, Yee SS, et al. Combining machine learning and nanofluidic technology to diagnose pancreatic cancer using exosomes. *ACS Nano* 2017;11(11):11182–11193. <https://doi.org/10.1021/acsnano.7b05503>.
- <sup>110</sup>Zhang C, Huo X, Zhu Y, et al. Electrodeposited magnetic nanoporous membrane for high-yield and high-throughput immunocapture of extracellular vesicles and lipoproteins. *Commun Biol* 2022;5(1):1358. <https://doi.org/10.1038/s42003-022-04321-9>.
- <sup>111</sup>Suwatthanarak T, Thiodorus IA, Tanaka M, et al. Microfluidic-based capture and release of cancer-derived exosomes via peptide-nanowire hybrid interface. *Lab Chip* 2021;21(3):597–607. <https://doi.org/10.1039/d0lc00899k>.
- <sup>112</sup>Dong J, Zhang RY, Sun N, et al. Bio-inspired NanoVilli chips for enhanced capture of tumor-derived extracellular vesicles: Toward non-invasive detection of gene alterations in non-small cell lung cancer. *ACS Appl Mater Interfaces* 2019;11(15):13973–13983. <https://doi.org/10.1021/acsmi.9b01406>.
- <sup>113</sup>Lim J, Choi M, Lee H, et al. Direct isolation and characterization of circulating exosomes from biological samples using magnetic nanowires. *J Nanobiotechnol* 2019;17(1):1. <https://doi.org/10.1186/s12951-018-0433-3>.



- <sup>114</sup>Zhou S, Hu T, Han G, et al. Accurate cancer diagnosis and stage monitoring enabled by comprehensive profiling of different types of exosomal biomarkers: Surface proteins and miRNAs. *Small* 2020;16(48):2004492. <https://doi.org/10.1002/sml.202004492>.
- <sup>115</sup>Li Z, Zhao J, Wu X, et al. A rapid microfluidic platform with real-time fluorescence detection system for molecular diagnosis. *Biotechnol Biotechnol Equip* 2019;33(1):223–230. <https://doi.org/10.1080/13102818.2018.1561211>.
- <sup>116</sup>Lin S, Yu Z, Chen D, et al. Progress in microfluidics-based exosome separation and detection technologies for diagnostic applications. *Small* 2020;16(9):1903916. <https://doi.org/10.1002/sml.201903916>.
- <sup>117</sup>Sharma P, Ludwig S, Muller L, et al. Immunoaffinity-based isolation of melanoma cell-derived exosomes from plasma of patients with melanoma. *J Extracell Vesicles* 2018;7(1):1435138. <https://doi.org/10.1080/20013078.2018.1435138>.
- <sup>118</sup>Sun N, Lee YT, Zhang RY, et al. Purification of HCC-specific extracellular vesicles on nanosubstrates for early HCC detection by digital scoring. *Nat Commun* 2020;11(1):4489. <https://doi.org/10.1038/s41467-020-18311-0>.
- <sup>119</sup>Liu LS, Wang F, Ge Y, Lo PK. Recent developments in aptasensors for diagnostic applications. *ACS Appl Mater Interfaces* 2021;13(8):9329–9358. <https://doi.org/10.1021/acscami.0c14788>.
- <sup>120</sup>Min L, Wang B, Bao H, et al. Advanced nanotechnologies for extracellular vesicle-based liquid biopsy. *Adv Sci* 2021;8(20):2102789. <https://doi.org/10.1002/adv.202102789>.
- <sup>121</sup>Jin D, Yang F, Zhang Y, et al. ExoAPP: Exosome-oriented, aptamer nanoprobe-enabled surface proteins profiling and detection. *Anal Chem* 2018;90(24):14402–14411. <https://doi.org/10.1021/acs.analchem.8b03959>.
- <sup>122</sup>Oh HJ, Kim J, Park H, Chung S, Hwang DW, Lee DS. Graphene-oxide quenching-based molecular beacon imaging of exosome-mediated transfer of neurogenic miR-193a on microfluidic platform. *Biosens Bioelectron* 2019;126:647–656. <https://doi.org/10.1016/j.bios.2018.11.027>.
- <sup>123</sup>Tayebi M, Tavakkoli Yarak M, Yang HY, Ai Y. A MoS<sub>2</sub>-MWCNT based fluorometric nanosensor for exosome detection and quantification. *Nanoscale Adv* 2019;1(8):2866–2872. <https://doi.org/10.1039/c9na00248k>.
- <sup>124</sup>Zhang P, He M, Zeng Y. Ultrasensitive microfluidic analysis of circulating exosomes using a nanostructured graphene oxide/polydopamine coating. *Lab Chip* 2016;16(16):3033–3042. <https://doi.org/10.1039/c6lc00279j>.
- <sup>125</sup>Zhang P, Zhou X, He M, et al. Ultrasensitive detection of circulating exosomes with a 3D-nanopatterned microfluidic chip. *Nat Biomed Eng* 2019;3(6):438–451. <https://doi.org/10.1038/s41551-019-0356-9>.
- <sup>126</sup>Lim J, Kang B, Son HY, et al. Microfluidic device for one-step detection of breast cancer-derived exosomal mRNA in blood using signal-amplifiable 3D nanostructure. *Biosens Bioelectron* 2022;197:113753. <https://doi.org/10.1016/j.bios.2021.113753>.
- <sup>127</sup>Yang Q, Cheng L, Hu L, et al. An integrative microfluidic device for isolation and ultrasensitive detection of lung cancer-specific exosomes from patient urine. *Biosens Bioelectron* 2020;163:112290. <https://doi.org/10.1016/j.bios.2020.112290>.
- <sup>128</sup>Singh K, Nalabotla R, Koo KM, Bose S, Nayak R, Shiddiky MJA. Separation of distinct exosome subpopulations: Isolation and characterization approaches and their associated challenges. *Analyst* 2021;146(12):3731–3749. <https://doi.org/10.1039/d1an00024a>.
- <sup>129</sup>Zhu L, Wang K, Cui J, et al. Label-free quantitative detection of tumor-derived exosomes through surface plasmon resonance imaging. *Anal Chem* 2014;86(17):8857–8864. <https://doi.org/10.1021/ac5023056>.
- <sup>130</sup>Im H, Shao H, Park YI, et al. Label-free detection and molecular profiling of exosomes with a nano-plasmonic sensor. *Nat Biotechnol* 2014;32(5):490–495. <https://doi.org/10.1038/nbt.2886>.
- <sup>131</sup>Yang KS, Im H, Hong S, et al. Multiparametric plasma EV profiling facilitates diagnosis of pancreatic malignancy. *Sci Transl Med* 2017;9(391):eaal3226. <https://doi.org/10.1126/scitranslmed.aal3226>.
- <sup>132</sup>Wang Y, Mao Z, Chen Q, Koh K, Hu X, Chen H. Rapid and sensitive detection of PD-L1 exosomes using Cu-TCPP 2D MOF as a SPR sensitizer. *Biosens Bioelectron* 2022;201:113954. <https://doi.org/10.1016/j.bios.2021.113954>.
- <sup>133</sup>Lim CZJ, Zhang Y, Chen Y, et al. Subtyping of circulating exosome-bound amyloid  $\beta$  reflects brain plaque deposition. *Nat Commun* 2019;10(1):1144. <https://doi.org/10.1038/s41467-019-09030-2>.
- <sup>134</sup>Pan S, Zhang Y, Natalia A, et al. Extracellular vesicle drug occupancy enables real-time monitoring of targeted cancer therapy. *Nat Nanotechnol* 2021;16(6):734–742. <https://doi.org/10.1038/s41565-021-00872-w>.
- <sup>135</sup>Teh Sk., Zheng W, Ho KY, Teh M, Yeoh KG, Huang Z. Diagnostic potential of near-infrared Raman spectroscopy in the stomach: Differentiating dysplasia from normal tissue. *Br J Cancer* 2008;98:457–465. <https://doi.org/10.1038/sj.bjc.6604176>.
- <sup>136</sup>Austin LA, Osseiran S, Evans CL. Raman technologies in cancer diagnostics. *Analyst* 2016;141:476. <https://doi.org/10.1039/c5an01786f>.
- <sup>137</sup>Jalali M, Isaac Hosseini I, AbdelFatah T, et al. Plasmonic nanobowtiefluidic device for sensitive detection of glioma extracellular vesicles by Raman spectrometry. *Lab Chip* 2021;21(5):855–866. <https://doi.org/10.1039/d0lc00957a>.
- <sup>138</sup>Wang J, Kao YC, Zhou Q, et al. An integrated microfluidic-SERS platform enables sensitive phenotyping of serum extracellular vesicles in early stage melanomas. *Adv Funct Mater* 2022;32(3):2010296. <https://doi.org/10.1002/adfm.202010296>.
- <sup>139</sup>Kim WH, Lee JU, Jeon MJ, Park KH, Sim SJ. Three-dimensional hierarchical plasmonic nano-architecture based label-free surface-enhanced Raman spectroscopy detection of urinary exosomal miRNA for clinical diagnosis of prostate cancer. *Biosens Bioelectron* 2022;205:114116. <https://doi.org/10.1016/j.bios.2022.114116>.
- <sup>140</sup>Li TD, Zhang R, Chen H, et al. An ultrasensitive polydopamine bifunctionalized SERS immunoassay for exosome-based diagnosis and classification of pancreatic cancer. *Chem Sci* 2018;9(24):5372–5382. <https://doi.org/10.1039/c8sc01611a>.
- <sup>141</sup>Dong S, Wang Y, Liu Z, et al. Beehive-inspired macroporous SERS probe for cancer detection through capturing and analyzing exosomes in plasma. *ACS Appl Mater Interfaces* 2020;12(4):5136–5146. <https://doi.org/10.1021/acscami.9b21333>.
- <sup>142</sup>Hsieh K, Patterson AS, Ferguson BS, Plaxco KW, Soh HT. Rapid, sensitive, and quantitative detection of pathogenic DNA at the point of care through microfluidic electrochemical quantitative loop-mediated isothermal amplification. *Angew Chem Int Ed* 2012;51(20):4896–4900. <https://doi.org/10.1002/anie.201109115>.
- <sup>143</sup>Wang Y, Xu H, Luo J, et al. A novel label-free microfluidic paper-based immunosensor for highly sensitive electrochemical detection of carcinoembryonic antigen. *Biosens Bioelectron* 2016;83:319–326. <https://doi.org/10.1016/j.bios.2016.04.062>.
- <sup>144</sup>Zhou Q, Rahimian A, Son K, Shin DS, Patel T, Revzin A. Development of an aptasensor for electrochemical detection of exosomes. *Methods* 2016;97:88–93. <https://doi.org/10.1016/j.ymeth.2015.10.012>.
- <sup>145</sup>Huang R, He L, Xia Y, et al. A sensitive aptasensor based on a hemin/G-quadruplex-assisted signal amplification strategy for electrochemical detection of gastric cancer exosomes. *Small* 2019;15(19):1900735. <https://doi.org/10.1002/sml.201900735>.
- <sup>146</sup>Dong H, Chen H, Jiang J, Zhang H, Cai C, Shen Q. Highly sensitive electrochemical detection of tumor exosomes based on aptamer recognition-induced multi-DNA release and cyclic enzymatic amplification. *Anal Chem* 2018;90(7):4507–4513. <https://doi.org/10.1021/acs.analchem.7b04863>.
- <sup>147</sup>Mathew DG, Beekman P, Lemay SG, Zuilhof H, Le Gac S, van der Wiel WG. Electrochemical detection of tumor-derived extracellular vesicles on nanoindented electrodes. *Nano Lett* 2020;20(2):820–828. <https://doi.org/10.1021/acs.nanolett.9b02741>.
- <sup>148</sup>Kashefi-Kheyraadi L, Kim J, Chakravarty S, et al. Detachable microfluidic device implemented with electrochemical aptasensor (DeMEA) for sequential analysis of cancerous exosomes. *Biosens Bioelectron* 2020;169:112622. <https://doi.org/10.1016/j.bios.2020.112622>.
- <sup>149</sup>Románszki L, Varga Z, Mihály J, Keresztes Z, Thompson M. Electromagnetic piezoelectric acoustic sensor detection of extracellular vesicles through interaction with detached vesicle proteins. *Biosensors* 2020;10(11):173. <https://doi.org/10.3390/bios10110173>.
- <sup>150</sup>Wang C, Wang C, Jin D, et al. AuNP-amplified surface acoustic wave sensor for the quantification of exosomes. *ACS Sens* 2020;5(2):362–369. <https://doi.org/10.1021/acssensors.9b01869>.

- <sup>151</sup> Yan H, Li Y, Cheng S, Zeng Y. Advances in analytical technologies for extracellular vesicles. *Anal Chem* 2021;93(11):4739–4774. <https://doi.org/10.1021/acs.analchem.1c00693>.
- <sup>152</sup> Suthar J, Parsons ES, Hoogenboom BW, Williams GR, Guldin S. Acoustic immunosensing of exosomes using a quartz crystal microbalance with dissipation monitoring. *Anal Chem* 2020;92(5):4082–4093. <https://doi.org/10.1021/acs.analchem.9b05736>.
- <sup>153</sup> Wu G, Zhao Y, Li X, et al. Single-cell extracellular vesicle analysis by microfluidics and beyond. *TrAC Trends Anal Chem* 2023;159:116930. <https://doi.org/10.1016/j.trac.2023.116930>.
- <sup>154</sup> Ortega-Sanchez FG, Teresa V, Widmann T, et al. Microfluidic systems in extracellular vesicles single analysis. A systematic review. *TrAC Trends Anal Chem* 2023;159:116920. <https://doi.org/10.1016/j.trac.2023.116920>.
- <sup>155</sup> Ramirez MI, Amorim MG, Gadelha C, et al. Technical challenges of working with extracellular vesicles. *Nanoscale* 2018;10(3):881–906. <https://doi.org/10.1039/c7nr08360b>.
- <sup>156</sup> Chen M, Lin S, Zhou C, Cui D, Haick H, Tang N. From conventional to microfluidic: Progress in extracellular vesicle separation and individual characterization. *Adv Healthcare Mater* 2023;12(8):2202437. <https://doi.org/10.1002/adhm.202202437>.
- <sup>157</sup> Wang S, Khan A, Huang R, et al. Recent advances in single extracellular vesicle detection methods. *Biosens Bioelectron* 2020;154:112056. <https://doi.org/10.1016/j.bios.2020.112056>.
- <sup>158</sup> Riazanski V, Mauleon G, Lucas K, et al. Real time imaging of single extracellular vesicle pH regulation in a microfluidic cross-flow filtration platform. *Commun Biol* 2022;5(1):13. <https://doi.org/10.1038/s42003-021-02965-7>.
- <sup>159</sup> Kim D, Woo HK, Lee C, et al. EV-Ident: Identifying tumor-specific extracellular vesicles by size fractionation and single-vesicle analysis. *Anal Chem* 2020;92(8):6010–6018. <https://doi.org/10.1021/acs.analchem.0c00285>.
- <sup>160</sup> Tayebi M, O'Rourke R, Wong HC, et al. Massively multiplexed submicron particle patterning in acoustically driven oscillating nanocavities. *Small* 2020;16(17):2000462. <https://doi.org/10.1002/sml.202000462>.
- <sup>161</sup> Zhang P, Zhou X, Zeng Y. Multiplexed immunophenotyping of circulating exosomes on nano-engineered ExoProfile chip towards early diagnosis of cancer. *Chem Sci* 2019;10(21):5495–5504. <https://doi.org/10.1039/c9sc00961b>.
- <sup>162</sup> Li J, Sina AAI, Antaw F, et al. Digital decoding of single extracellular vesicle phenotype differentiates early malignant and benign lung lesions. *Adv Sci* 2023;10(1):2204207. <https://doi.org/10.1002/advs.202204207>.



**Xinyuan He** received a B.S. degree from Northwestern Polytechnical University in 2021, majoring in microelectromechanical systems engineering. He is currently pursuing an M.S. degree at Tianjin University. His research interests focus on microsystems-on-a-chip for separation and detection of extracellular vesicles based on high-frequency acoustofluidic technology.



**Wei Wei** received an M.S. degree from Tianjin University, Tianjin, China, in 2022, where he is currently pursuing the Ph.D. degree. His research interests focus on MEMS devices and acoustofluidics, especially for the manipulation of nanoparticles and bio-nanoparticles.



**Xuexin Duan** received a Ph.D. degree at University of Twente, Netherland (2010). After postdoctoral studies at Yale University, he moved to Tianjin University. Currently, he is a full professor at the State Key Laboratory of Precision Measuring Technology and Instruments, Department of Precision Instrument Engineering of Tianjin University. His research is on MEMS/NEMS devices, microsystems, and microfluidics, and their interfaces with chemistry, biology, medicine, and environmental science.